AD NUMBER

AD875901

LIMITATION CHANGES

TO:

Approved for public release; distribution is unlimited.

FROM:

Distribution authorized to U.S. Gov't. agencies and their contractors; Critical Technology; SEP 1970. Other requests shall be referred to U.S. Army Aviation Materiel Laboratories, Fort Eustis, VA 23604. This document contains export-controlled technical data.

AUTHORITY

USAAML ltr, 29 Mar 1971

(70)

AD

USAAVLABS TECHNICAL REPORT 70-43

FLIGHT VIBRATION AND ENVIRONMENTAL EFFECTS ON FORMATION OF COMBUSTIBLE MIXTURES WITHIN AIRCRAFT FUEL TANKS

Final Report

By
T. C. Kosvic
N. L. Holgeson
B. P. Breen

September 1970

U. S. ARMY AVIATION MATERIEL LABORATORIES
FORT EUSTIS, VIRGINIA

CONTRACT DAAJ02-69-C-0063
DYNAMIC SCIENCE
A DIVISION OF MARSHALL INDUSTRIES
IRVINE, CALIFORNIA

DISCLAIMERS

The findings in this report are not to be construed as an official Department of the Army position unless so designated by other authorized documents.

When Government drawings, specifications, or other data are used for any purpose other than in connection with a definitely related Government procurement operation, the United States Government thereby incurs no responsibility nor any obligation whatsoever; and the fact that the Government may have formulated, furnished, or in any way supplied the said drawings, specifications, or other data is not to be regarded by implication or otherwise as in any manner licensing the holder or any other person or corporation, or conveying any rights or permission, to manufacture, use, or sell any patented invention that may in any way be related thereto.

Trade names cited in this report do not constitute an official endorsement or approval of the use of such commercial hardware or software.

DISPOSITION INSTRUCTIONS

Destroy this report when no longer needed. Do not return it to the originator.

DEPARTMENT OF THE ARMY
U S ARMY AVIATION MATERIEL LABORATORIES
FORT EUSTIS, VIRGINIA 23604

This report was prepared by Dynamic Science under the terms of Contract DAAJ02-69-C-0063.

Under the contract, a fuel tank test fixture was fabricated and instrumented, and the fuel/air vapor mixture in the ullage of the tank was measured under various atmospheric, dynamic, and geometric conditions.

A fuel/air vapor gradient was found in the ullage. The range of the gradient was such that a flammable region was found under conditions considered to be safe from an equilibrium standpoint.

This command concurs with the conclusions set forth in this report.

Task 1F162203A15003
Contract DAAJ02-69-C-0063
USAAVLABS Technical Report 70-43
September 1970

FLIGHT VIBRATION AND ENVIRONMENTAL EFFECTS ON FORMATION OF COMBUSTIBLE MIXTURES WITHIN AIRCRAFT FUEL TANKS

Final Report

By

T. C. Kosvic
N. L. Helgeson
B. P. Breen

Prepared by

Dynamic Science
A Division of Marshall Industries
Irvine, California

for

U. S. ARMY AVIATION MATERIEL LABORATORIES
FORT EUSTIS, VIRGINIA

SUMMARY

The objective of this study was to determine fuel tank vapor space characteristics for a simulated helicopter fuel tank and to evaluate the potential hazard which exists. Fuel/air ratios were measured as a function of time and position within the ullage of the fuel tank for specified flight profiles. These results were compared to published flammability limits as a basis for assessing flight hazard potential. The flight profiles were simulated by withdrawing fuel (at rated engine usage) from a vibrating tank held at constant pressure and temperature. Parametric variations were made in fuel temperature (40° to 100°F), flight altitude (0 to 15,000 feet), vibration environment, and fuel properties (liquid JP-4 versus JP-4 emulsion EF4-104H). Another important variable not considered initially but which was uncovered during the course of this investigation was the effect that the rubberized tank liner (FF-10056) could have on the measured fuel/air ratios. The extent of this effect was found to be related to fuel temperature and exposure time of the liner to the fuel.

The experimental results showed those ranges of the test variables which had a significant effect on the measured fuel/air ratios. They also demonstrated that fuel/air mixture gradients do exist in fuel tanks under flight conditions. It was found that tanks which would be considered safe as determined by calculations for equilibrium conditions actually contain flammable regions, even for level flight. An analytical model for the ullage space was written which included transient fuel vapor diffusion and convection which was brought about by venting of the ullage. The sample cases gave results which showed reasonable agreement in both shape and magnitude with the measured composition profiles.

FOREWORD

This final report documents the work performed by the Dynamic Science Division of Marshall Industries, Irvine, California. This effort was sponsored by the U.S. Army Aviation Materiel Laboratories, Fort Eustis, Virginia, under Contract DAAJ02-69-C-0063, Task 1F162203A15003, and was monitored technically by Lt. Charles Pedriani, who made substantial technical contributions based on related work.

The authors wish to thank Mr. Arlen Bell, who conceived, designed, and supervised construction of the vibration table and experimental fuel tanks. Also, Miss Mary Ann McLain and Mr. John R. White must be acknowledged for valuable assistance in running the test series and Dr. R. H. Kratzer for performing the deaeration of JP-4 fuel.

TABLE OF CONTENTS

LIST OF ILLUSTRATIONS

INTRODUCTION

Helicopters become increasingly vulnerable to ballistic hits in fuel tank areas when the vapor space above the fuel contains flammable fuel/air mixtures. Although the equilibrium fuel/air ratio (calculated from vapor pressure at fuel temperature and total pressure) is often too fuel-rich to support an ignition, there exist transient fuel/air gradients of air near the tank vent and a rich fuel/air mixture below. This region of air is brought about by air entering the vent due to engine usage, center-of-gravity adjustment, or changes in altitude. Somewhere in this region of mixture gradients, an ignitable/explosive layer exists, and as this layer gets larger (involves a larger quantity of the ullage gas), the helicopter is rated as more vulnerable to ground fire or accident. Penetration of the tank by an incendiary projectile under these conditions can result in a catastrophic loss of the aircraft.

Many methods have been proposed to reduce this vulnerability, including: armor-plating to protect tanks; use of pressurized tanks, which would maintain a very full rich (and therefore incombustible) mixture; inerting with nitrogen or inert gas (presaturation of fuel followed by tank treating in flight); and use of a collapsible tank liner to eliminate the vapor space. All of these methods add weight to the helicopter structure and therefore decrease payload and/or range and are not considered satisfactory. This study was undertaken to obtain a more fundamental understanding of fuel tank mixing dynamics in the hope that new methods for eliminating the hazard imposed by flammable/explosive mixtures may be realized. This program was undertaken as a first step to identify the controlling phenomena causing fuel/air mixture gradients.

To date, very little is known about the mixture gradients existing within fuel tanks. Gradients were known to exist, but very little data showing quantitative influences of aircraft operational and structural characteristics were available. Data have been reported by Nestor (Reference 1) showing explosive limits of fuel vapors as a function of liquid temperature and aircraft altitude. These data were for conditions of essentially equilibrium mixtures throughout the vapor space. Gradients of mixture ratio were not considered. There are other investigations (e.g., Reference 2) where knowledge of the fuel/air ratio within the ullage would have been useful, but for a variety of reasons it was not measured. The primary objectives of this study were to demonstrate that fuel/air mixture gradients did exist and to determine the relative effect that flight/aircraft parameters had on the magnitude of fuel/air gradients.

To accomplish these objectives, a three-phase program was initiated. Phase I consisted of the design, fabrication, assembly, and checkout of the test apparatus. This equipment consisted of a vibration table and experimental fuel tank within which fuel/air gradients were measured. The basic system included fuel and fuel transfer tanks, a vibration table, a fuel temperature conditioning system, and instrumentation and lines for sampling and analyzing samples from the vapor space.

In Phase II (Test Program), composition profiles within the ullage were determined for several parameters as a function of time and position. Those considered were liquid fuel temperature, flight altitude, level of agitation, and fuel type (JP-4 and emulsion EF4-104H). An additional influencing parameter discovered during the course of testing was the exposure time/temperature characteristics for saturated rubber-lined tanks. All tests were conducted using a level flight profile; that is, constant-altitude tests were run from sea level to 15,000 feet. Ascents and descents were not considered in this program, but they are important considerations for future tests. The effect of fuel withdrawn for engine usage was included in all tests.

Phase III (Analysis of Test Data) was conducted to determine the effect of test parameters on the composition profile within the ullage. A mathematical diffusion/convection model was developed, and sample cases were calculated for comparison with test data. The calculated profiles agreed quite favorably and exhibited similar trends as the experimental data.

As a result of this study, the relative effects of the test parameters were determined under constant altitude and constant withdrawal rates. Furthermore, it was demonstrated that fuel tanks that are considered to be safe from an equilibrium point of view do in fact contain flammable regions caused by a fuel vapor gradient phenomenon.

TECHNICAL DISCUSSION

The purpose of this discussion is to provide a technical background summary upon which the interpretation of the experimental data can be made. The general test procedure of a simulated flight profile begins with the fuel tank full of fuel to within 6 or 7 inches from the top. The tank pressure is then brought to correspond to a selected simulated altitude and held there throughout the test. As the test proceeds, the fuel is withdrawn at a nominal rate of 1 gpm which causes the fuel level to change at a rate of 1/4 inch per minute(in large tank only). This withdrawal rate is representative of actual helicopter flight requirements. As the fuel is withdrawn, the space which the liquid previously occupied is filled with a fuel vapor and air mixture. The air is drawn in primarily through the vent of the fuel tank. When the helicopter is at altitude, however, conditions exist so that the amount of air dissolved in the fuel may exceed the equilibrium value. When this occurs, the dissolved air begins to evolve from the liquid as bubbles and it passes into the vapor space. The fuel vapor, for the most part, comes from evaporation from the liquid fuel surface, but it may also come from evaporation of liquid absorbed in the walls of the rubberized tank lining material.

As the vent air and fuel vapors enter the vapor space (ullage), a mixing/diffusion process is initiated which starts to eliminate the concentration gradients that have developed (see Figure 1(a)). This mixing may involve several modes of transport: molecular diffusion, turbulent diffusion, free convection, interphase mass transfer, or a combination of any of these. Depending upon the modes of transport involved, in any particular case, the mixing process may take place rapidly (minutes) or slowly (hours). As a result, large fuel/air concentration gradients can develop in the ullage space for some conditions and uniform mixtures may exist at others. This discussion is presented to help determine when these various phenomena become important and to determine how they affect the fuel-air gradients within the ullage space of the fuel tank.

LEVEL FLIGHT PROFILE

The process of replacing the consumed fuel with a fuel/air mixture is shown schematically in Figure 1(b). The top of the tank remains stationary and the liquid fuel surface recedes from it at a velocity v_s. We assume that the entire top of the tank is a vent; therefore, as the liquid recedes, fuel-free air enters the top of the tank in a uniform stream at a velocity v_t. The air will enter the top of the fuel tank at the same velocity as the fuel is receding ($v_t = v_s$) if there is no supply of fuel vapors or air fed into the vapor space from the liquid or the walls of the fuel tank. We have assumed that the air enters in a uniform stream. That is, we have neglected the fact that the air actually enters at a single point, the vent opening, and then spreads out by diffusion and convection into approximately horizontal layers. Experimental results showed (see later section) that this is what appeared to be happening.

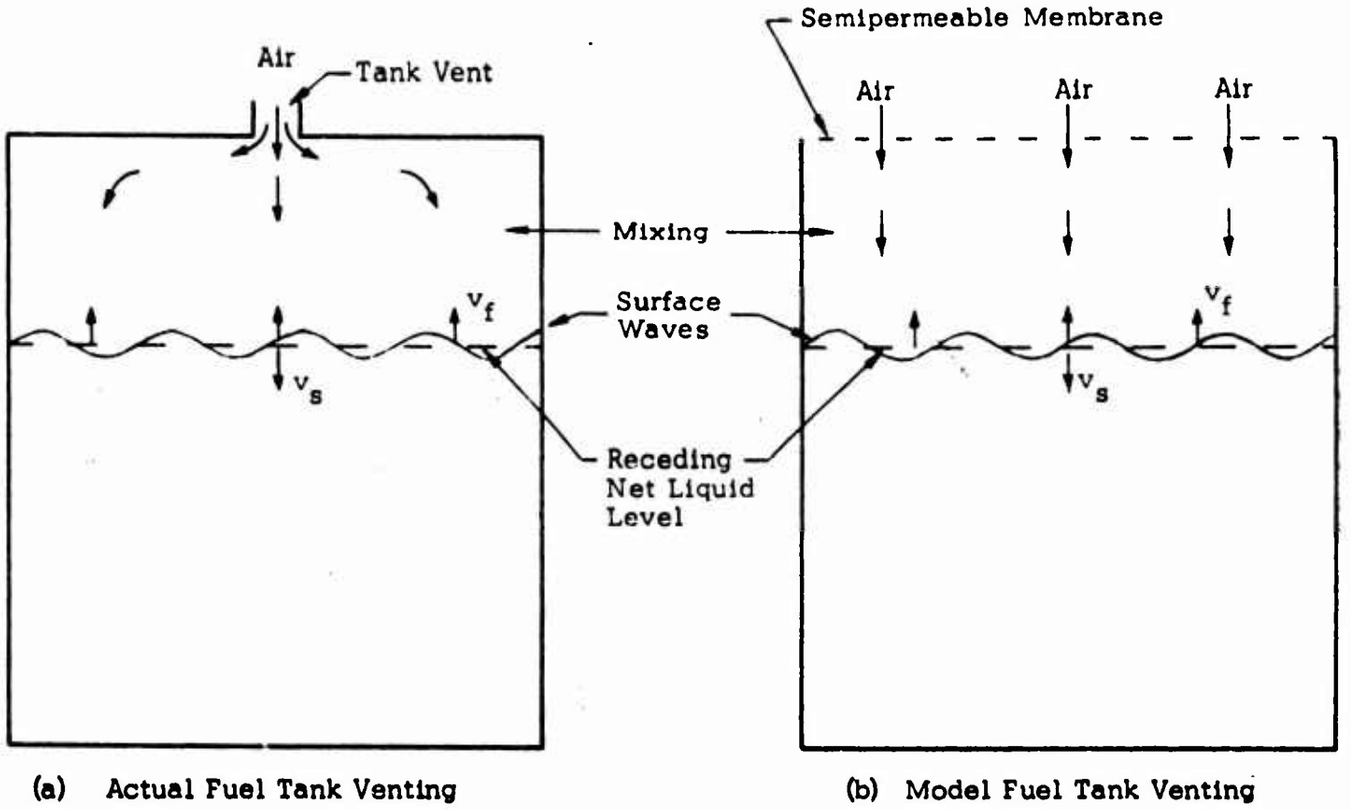

Figure 1. Comparison of Actual and Model Fuel Tank Venting.

Fuel vapors cannot escape from the tank unless their transport velocity is higher than the vent air velocity. We can, therefore, make one additional approximation, which will help in understanding the experimental results: the tank top is a nearly semipermeable membrane; that is, air can flow through in one way, but the fuel vapors cannot diffuse through it in the opposite direction.

We also introduce a third velocity (v_f) which characterizes the bulk flow of fuel vapors and possibly air that emerges from the fuel. (The origin of the term $N_{f,o}$ is discussed in greater detail in Appendix IV.)

$$v_f = \frac{N_{f,o} + N_{a,o}}{c}$$

Here $N_{f,o}$ is the molar flux (moles/area-time) of fuel vapors and $N_{a,o}$ is the molar flux of air emerging from the surface of the fuel. They are measured relative to the fuel surface. One or both of these fluxes may be important in a given test. Whenever there is diffusion of fuel vapors away from the liquid surface into the ullage, $N_{f,o} > 0$. This quantity becomes increasingly significant as the composition at the surface of the liquid gets richer (high fuel temperature, low ambient pressure). $N_{a,o}$ would generally not be important for conditions at or near sea level. If the ambient pressure changes significantly, however, air previously dissolved in the fuel will come out of solution as the ambient pressure is decreased. (c) is the total molar density (moles/volume) of the vapor phase. We may write an equation relating these three velocities:

$$v_t = v_s - v_f \tag{1}$$

If v_f is zero (or small), $v_t \approx v_s$ as mentioned previously. Any increase in the value of v_f retards the rate at which air will enter the top of the fuel tank; as v_f gets larger, v_t eventually becomes negative. That is, there could be bulk flow of material out of the top of the tank in spite of the fact that fuel is being consumed by the aircraft engine. This result accounts for evaporative loss from aircraft at high altitude.

The effect of the relative values of these velocities (v_t, v_s, and v_f) on the composition profile within the ullage is illustrated in Figure 2. The time, t_o, indicates the initial conditions of the test where the vapor space is essentially at equilibrium (i.e., flat composition profile). Times t_1, t_2, and t_3 are progressions of time during the test which show the development of composition profile with time.

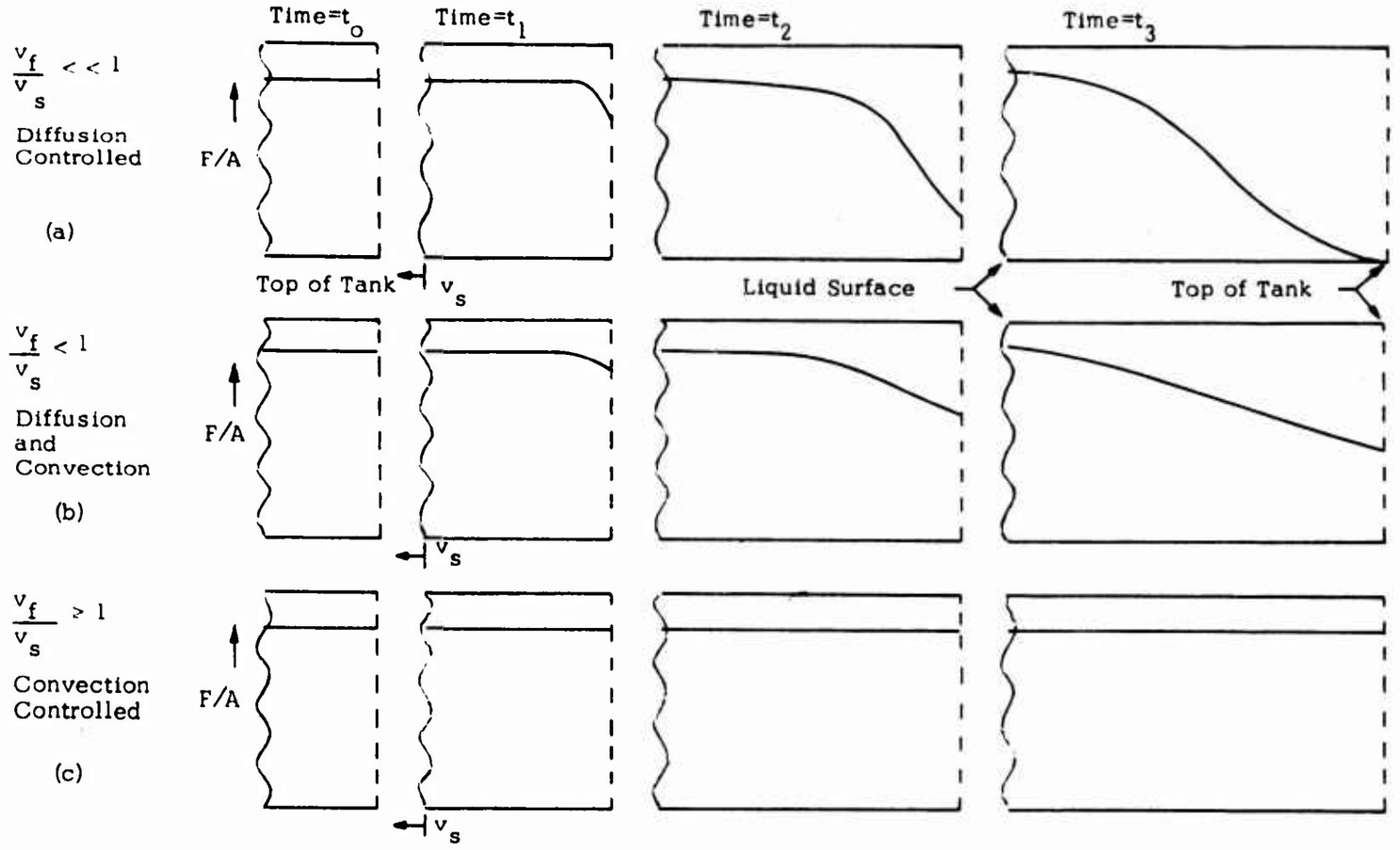

Figure 2. Illustrative (Fuel/Air) Composition Profiles in Ullage Volume as a Function of Time for Variable v_f/v_s.

In part (a) of Figure 2, $v_f/v_s << 1$, so that $v_t \approx v_s$. Here a completely diffusive transport mechanism for transport of fuel vapors from the liquid surface to the top of the ullage may be anticipated. As time progresses from t_o to t_3, the surface of the liquid fuel recedes from the top of the fuel tank. The concentration at the surface of the fuel is constant and is determined by the vapor pressure of the fuel and the tank pressure. The fuel vapors are supplied to the top of the tank by diffusion from the surface of the fuel but then do not diffuse out of the tank. As the additional air enters the top of the tank, the concentration of fuel vapors at the top of the tank continues to decrease.

Figure 2(b) illustrates the case for $v_f/v_s <$. As v_f increases, transport of fuel vapors to the top of the ullage becomes convective controlled rather than diffusive. The composition profile tends to flatten out as the flow of air and fuel vapor passing into the ullage at the liquid surface becomes important.

If v_f becomes greater than v_s, a convective motion of the mixture is set up so that material is now flushed out of the ullage through the vent (Figure 2(c)) and no fresh air is permitted to enter the ullage. Considered in this manner, the ratio v_f/v_s becomes a qualitative measure of the effect of a convective motion generated by interphase mass transfer (evaporation of fuel and dissolution of air) on composition profiles within the vapor space. This classification of the controlling phenomena (diffusion/convection) will help in presenting an analysis descriptive of fuel tank behavior.

Model for Diffusion Transport

Assuming that the fuel/air mixture is of two components, one fuel species and one air species, the equation of continuity for fuel species may be written as (Reference 3)

$$N_f = \underbrace{X_f (N_f + N_a)}_{\text{convection}} - \underbrace{c\, D_{fa}\, \nabla X_f}_{\text{diffusion}} \qquad (2)$$

where N_f = molar flux/unit time relative to liquid surface

X_f = mole fraction components

c = total molar concentration/volume

D_{fa} = binary diffusion coefficient for fuel vapors in air

The quantity $(N_A + N_B)$ represents a bulk convective flow and is measured relative to the liquid surface. For an open system some bulk flow will exist in the vapor phase as long as a concentration gradient exists. However, for the case under consideration (diffusion controlled), it is sufficiently small to be negligible. Equation (2) becomes

$$N_f = c\, D_{fa}\, \nabla X_f \Big\} \text{ Diffusion control} \qquad (3)$$

and using the continuity relation

$$\frac{\partial c_f}{\partial t} = c \frac{\partial X_f}{\partial t} = -\nabla N_f$$

differentiating and substituting in equation (3),

$$\frac{\partial X_f}{\partial t} = D_{fa} \nabla^2 X_f \tag{4}$$

This is Fick's second law of diffusion, which can be solved for a variety of initial and boundary value problems. At this point we are interested in the situation illustrated in Figure 2(a) ($v_f/v_s << 1$). For this case, the initial and boundary conditions are (see Figure 3 for coordinate system):

$$\begin{aligned} t = 0 \quad & X_f(z,0) = X_{f,o} = X_{f,e} \\ t > 0 \quad & \frac{\partial X_f}{\partial z}(L,t) = f(t) \\ & X_f(o,t) = X_{f,o} = X_{f,e} \end{aligned} \tag{5}$$

where $L = L(t) = A + v_s t$

The subscript o refers to the condition at the liquid surface, L refers to the top of the tank, and e signifies an equilibrium concentration. The feature that makes these conditions rather unique is that one of the boundaries (L) is moving at a steady rate to simulate the receding liquid surface. It should also be noted that the boundary condition at L(t) is an unspecified function of time f(t). The gradient at this position (the semipermeable membrane) is not zero, as a steady supply of fuel vapors is required to mix with the incoming air and is subsequently swept back into the tank. This gradient is estimated by use of the experimental data. Using these results, a generating function for this boundary condition as a function of time is established.

Analytical solutions for equation (4) for these conditions are not available; however, equation (4) and the tank top boundary condition were programmed using an adaption of a Thermal Analyzer Computer program converted for diffusion with the addition of the vent air convection terms. Solutions were calculated using a CDC 6400 computer. The calculated composition profiles are shown in Figures 5 through 7 for fuel temperatures of 46°, 60°, and 107°F corresponding to experimental tests. These results are compared to the experimental measurements in a later section.

For the intermediate case of $v_f/v_s < 1$ (Figure 2(b)), the model is slightly less accurate. The terms $N_{f,o}$ and $N_{a,o}$ (bulk fuel convection) must be evaluated. This was not considered to be within the scope of the present program, however, and calculations for this case have not be completed. In the last case (Figure 2(c)), a diffusion mechanism is not involved; transport is entirely by convection.

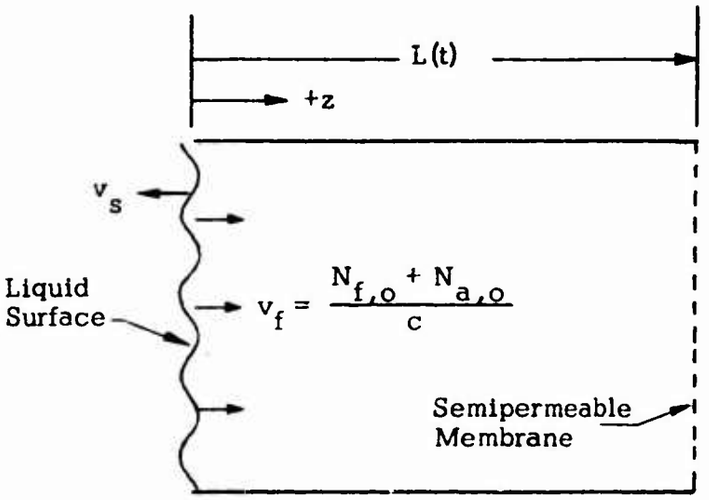

Figure 3. One-Dimensional Coordinate System for Moving Boundary Calculations.

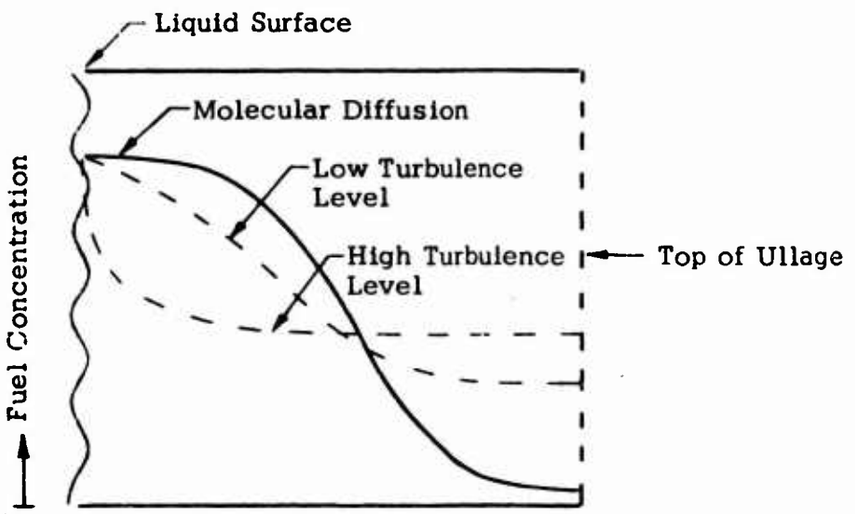

Figure 4. Effect of Diffusion Coefficient on Composition Profiles Within Ullage.

At this point it is pertinent to discuss how the the experimental test variables may affect v_f which, in turn, affects the experimental results.

Agitation

The calculated composition profile shown in Figures 5 through 7 assumed that transport of fuel vapors from the liquid surface was entirely by molecular diffusion from a flat, smooth, liquid surface. In practically all of the tests conducted, the fuel tank was subjected to a forced vibration to simulate actual aircraft environment (see section on experimental equipment). This caused the surface to ripple and to break into waves (3 to 4 inches in height, peak-to-peak), which sloshed back and forth within the fuel tank. The wave motion will induce certain mixing and convection phenomena in the ullage which would not exist in an undisturbed fuel tank. Thus, rather than a molecular diffusion occurring, a turbulent mixing mechanism dominates near the surface of the liquid. However, this turbulence need not extend throughout the ullage space; in fact, it may decay rather quickly so that in the upper parts of the ullage molecular diffusion is the important transport mechanism. In this sense, a more realistic diffusion coefficient to be used in future calculations may be one that is a function of position: very high ($\approx$ 100 ft^2/hr) near the surface of the liquid and low (0.3 ft^2/hr) near the top of the fuel tank.

The effect of increasing the value of the diffusion coefficient (D_{a_f}) is to cause the gradient profile to develop much more rapidly (see Figure 4); that is, a turbulent mechanism tends to eliminate gradients within the turbulent medium. A series of curves was calculated again using the computer model, increasing the diffusion coefficient by a factor of 3. No differences of the composition profiles were observed. Therefore, large changes in the diffusion coefficient are required if appreciable changes in the composition profiles are to be seen (factor of 20 to 100 increase in diffusion coefficient). Changes of this order could be realized, possibly under flight conditions of extreme turbulence.

Three-Dimensional Effects

The calculations discussed above assume a one-dimensional model. The experimental measurements presented later are also one-dimensional in that all fuel/air samples were taken on a vertical line close to the center of the ullage. The sides and corners of the ullage were not sampled. The analytical calculations assumed that the velocity profile of the air coming into the vent was that of a one-dimensional stagnation flow field, i.e., the velocity decreasing linearly to zero at the liquid surface. The data seem to indicate that this is what happened with unlined tanks.

Under certain conditions of fuel temperature and pretest exposure time of the liquid fuel to a lined tank, the data indicate that the liquid surface was not the only source of fuel vapor. Three-dimensional effects due to evolution of fuel vapors from a rubber-lined tank usually tended to increase the effect of v_f and reduce the gradients within the ullage space.

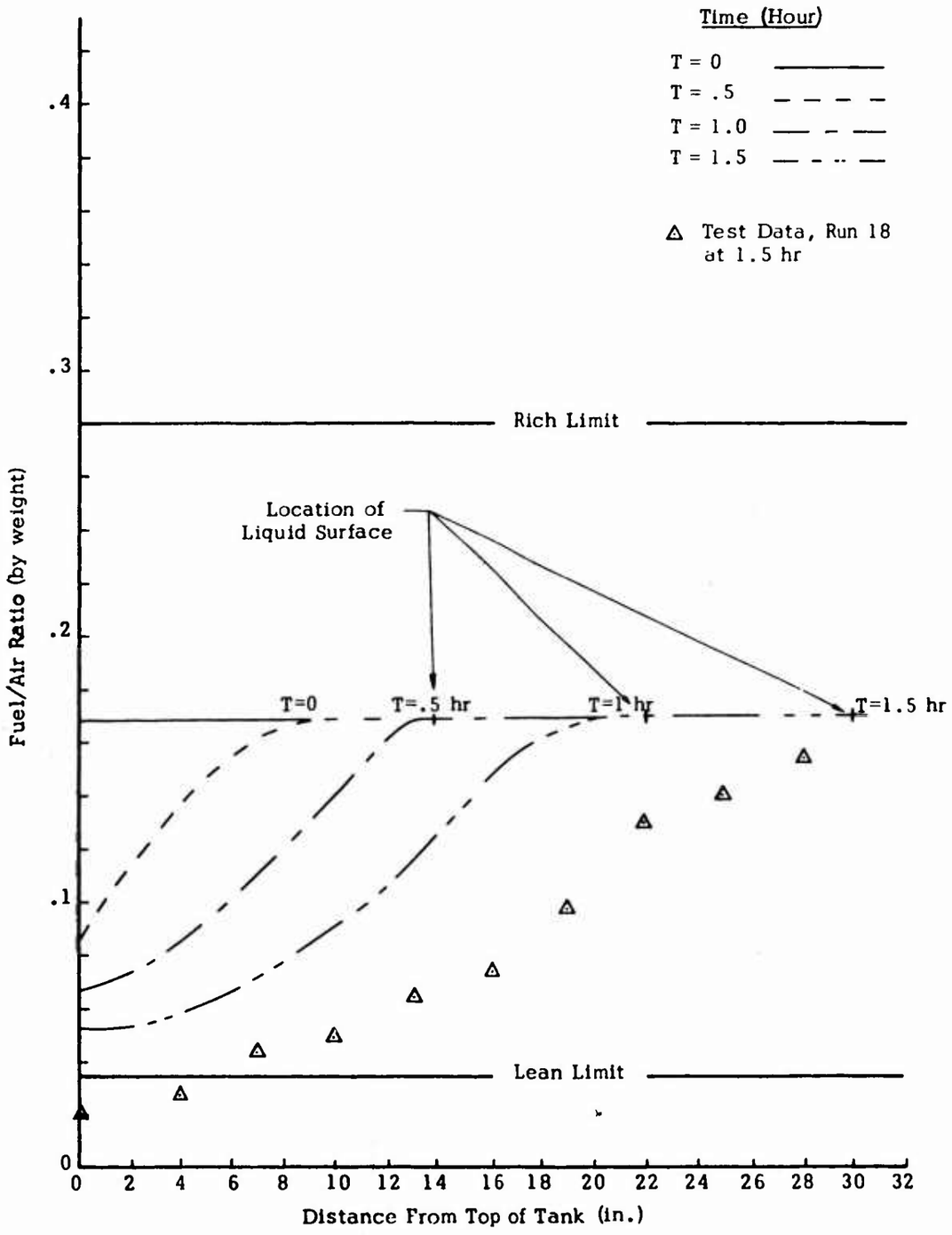

Figure 5. Diffusion/Convection Program Results for JP-4 at 46° F.

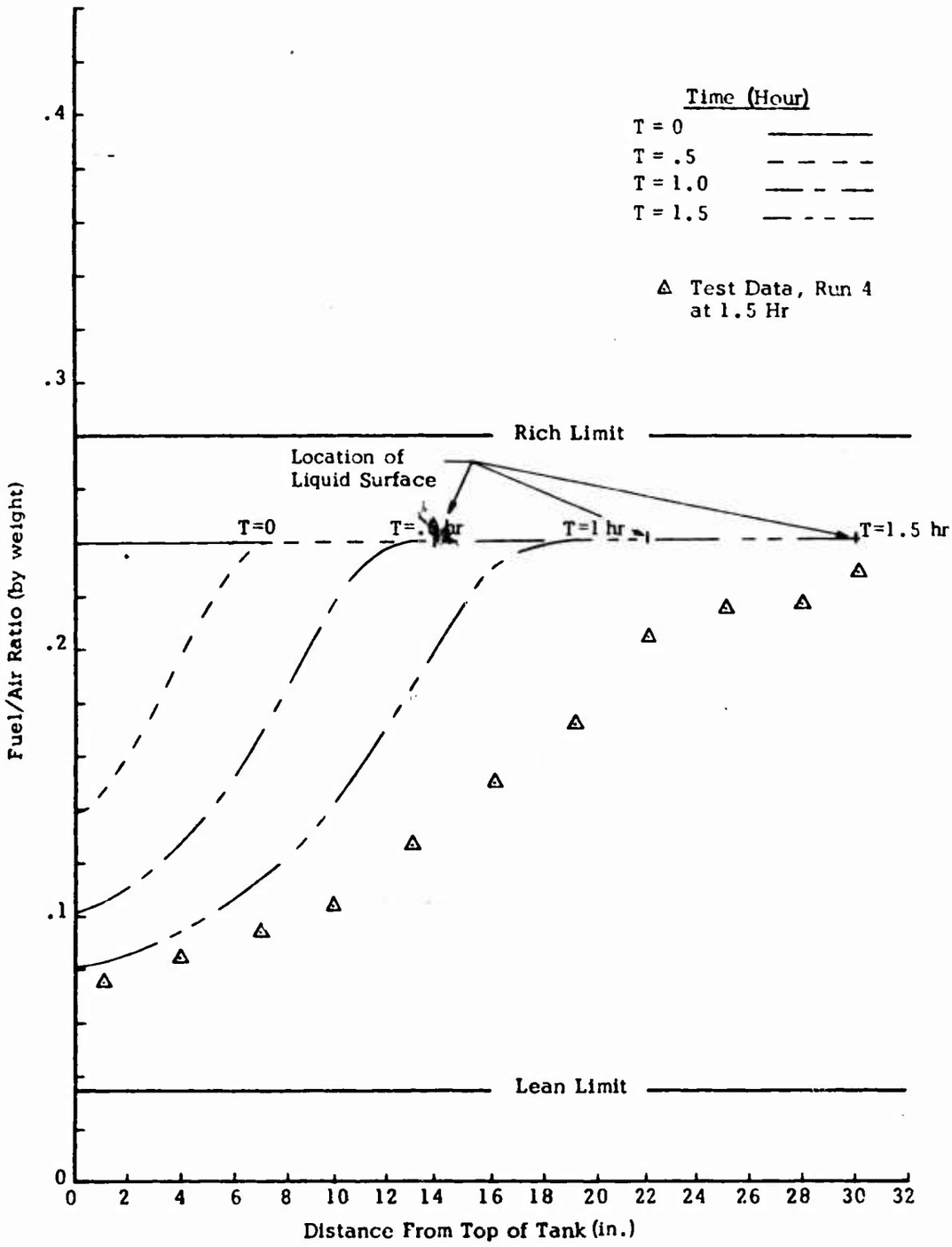

Figure 6. Diffusion/Convection Program Results for JP-4 at 60° F.

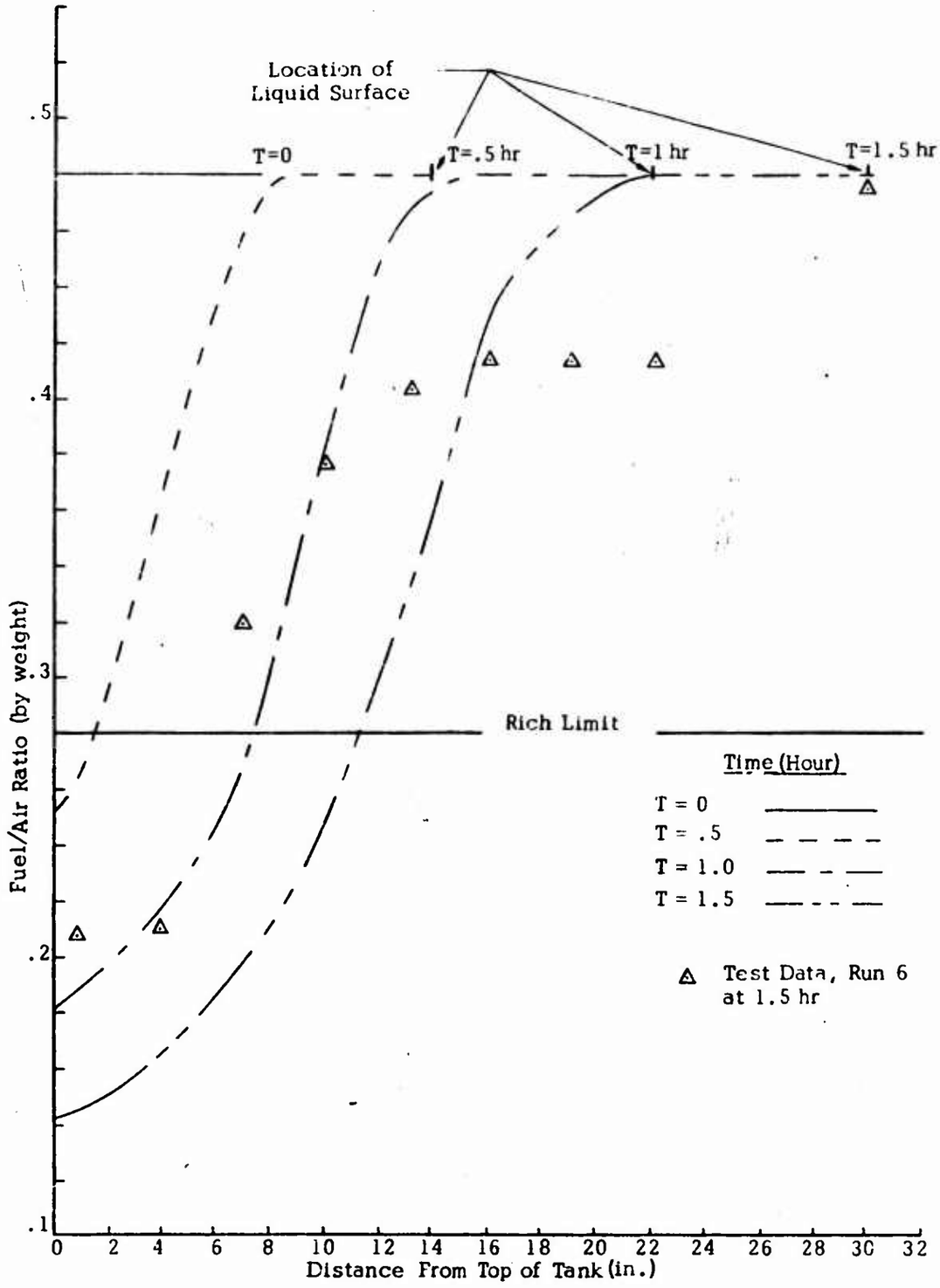

Figure 7. Diffusion/Convection Program Results for JP-4 at 107° F.

Fuel Type

Two types of fuel were considered in this program: JP-4 and emulsion (EF-104H). Ordinarily, the major difference for different fuels would be their vapor pressure. In this case, flow properties must also be considered. Agitation of the fuel tank would be expected to have only relatively minor effects on the condition of the surface of the emulsion fuel. Very minor, if any, rippling and wave motion would be expected.

DESCENT FLIGHT PROFILE

The previous discussion was concerned with evaluating the phenomena that exert an important effect on fuel/air gradients while the aircraft is in level flight. In this section, the additional effect of descent of the aircraft is considered in a less detailed treatment.

Consider the case of the aircraft flying at an altitude of 15,000 feet (.5 atmosphere) and descending at 1500 ft/min from 15,000 feet. The velocity of the air entering the ullage of the fuel tank is controlled not only by the rate of fuel consumption of the aircraft, but primarily by the rate of pressurization of the ullage space. The pressure within the fuel tank approximately doubles as the aircraft descends to sea level, and therefore the original mixture is compressed to one-half of its volume. If we take the ullage to have a mean depth of 2 feet during the descent, air would enter the ullage and occupy one-half of this thickness (12 inches) by the time the aircraft had descended to sea level. These conditions result in an equivalent velocity of air entering the tank (v_t) of 1.2 inches/minute, which is a factor of five times the velocity (v_t = .25 inch/min) induced by fuel consumption. The effect that this rapid influx of air may have on the composition profile is shown in Figure 8.

As the mixture originally present in the ullage is compressed, the partial pressure of the fuel vapors near the liquid surface starts to exceed the vapor pressure of the fuel for that temperature, and condensation starts to occur. A sharp break in the concentration profile will exist at the interface between the incoming air and the original mixture, because very little diffusion will have taken place in the ten minutes required for the aircraft to descend.

An equation similar to equation (1) may now be written for the descent case.

Using the mass balance below:

$$\frac{d(\rho V_{ull})}{dt} = \rho \frac{dV_{ull}}{dt} + V_{ull} \frac{d\rho}{dt} = \dot{m}_t + \dot{m}_f$$

$$\dot{m}_t = \rho_a v_t A, \quad \dot{m}_f = \rho_f v_f A, \quad V_{ull} = AL$$

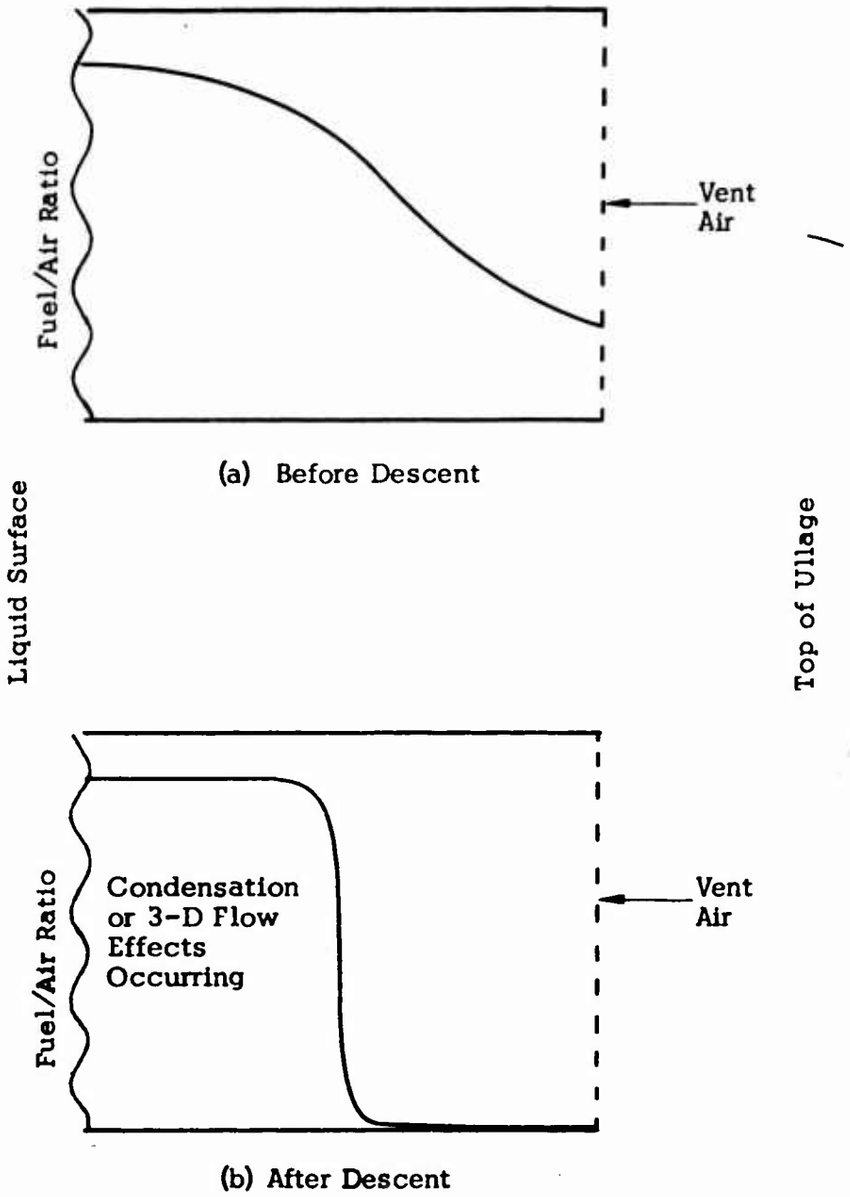

Figure 8. Comparison of Composition Profiles Before and After Descent of Helicopter From 15,000 Feet to Sea Level.

where $\dot{m}_f$ = mass flow rate of fuel into ullage

$\dot{m}_t$ = mass flow rate of air into ullage

V_{ull} = volume of ullage

ρ = density of vapor mixture

ρ_a = density of air entering tank

ρ_f = density of fuel entering ullage

A = cross-sectional area of tank

L = vertical dimension of ullage

v_t = velocity of air into top of tank

M_a = molecular weight of air

M_f = molecular weight of fuel

Assuming the instantaneous air/fuel ratio (A/F) is known and is temperature constant within the tank, the gas law yields

$$(A/F) = \frac{\rho_a}{\rho_f} = \frac{M_a P_a}{M_f P_f}$$

The mixture density is then $\rho = \rho_a + \rho_f = \rho_f(1 + (A/F))$.

Substitution into the mass balance yields

$$\dot{m}_t = \rho A \frac{dL}{dt} + AL \frac{d\rho}{dt} - \dot{m}_f$$

or

$$v_t = \left[\frac{(1+(A/F))}{(A/F)}\right] v_s + L \frac{1}{\rho_a} \frac{d}{dt} \rho_f(1+(A/F)) - \frac{v_f}{(A/F)}$$

where v_s is defined as the surface recession rate dL/dt.

This equation is similar to equation (1) but includes an additional term which accounts for a velocity into the ullage due to the descent. The usefulness of this relation is that it tells us the conditions under which no tank air is permitted into the fuel tank through the vent. That is, if a sufficiently high value of v_f can be generated by some device within the tank, v_t becomes negative and air is not permitted into the ullage through the vent.

EXPERIMENTAL PROGRAM

The basic theme of this work was to assess helicopter fuel tank vulnerability characteristics at nonequilibrium conditions associated with the aircraft environment. (The assessment of vulnerability was related to the ratio of tank ullage volume within flammable ranges to the total ullage volume.) Flight parameters evaluated during the program were vibration frequency, altitude (tank pressure), and fuel temperature. Aircraft/fuel parameters varied were fuel type (liquid JP-4 versus emulsified JP-4), tank liner materials, and tank geometry. The equipment,when assembled, included a vibration table, simulated helicopter fuel tanks, and measuring instrumentation. This section describes in detail the experimental equipment, test procedures, instrumentation, and test results.

EXPERIMENTAL EQUIPMENT

Figure 9 shows the basic test setup. It consists of four separate systems: the vibration table, fuel tank and transfer system, fuel temperature conditioning system, and fuel sampling system.

Vibration System

The vibration system (Figure 10) consists of an outer support frame and an inner vibration table that are connected by two spring bars. Input force is generated by a LAB mechanical vibration generator (Model LIGHT B) powered by a 1-hp DC motor with a flexible shaft drive. The vibrator is of the reaction type with counterrotating adjustable steel eccentric weights. The generator has two shafts which are geared together so that the centrifugal force vectors of the individual shafts are resolved into a rectilinear force that produces straight-line vibrations in a line normal to the plane in which the shaft axes lie. In Figures 9 and 10, the generator is shown mounted beneath the vibration table. Output force of the generator applied to the vibration table and all other spring masses then varies as the square of the frequency.

Test frequencies required in the test program ran from 310 cpm to 3500 cpm. These are typical of flight vibration levels encountered in helicopter flights. The force output from the vibration generator at low frequencies is insufficient to drive the total sprung weight (sum of weights of vibration table, full fuel tank, transfer tanks, and vibration generator) at the required g level (.15g). It is necessary to "tune" the spring bar system so that its natural frequency matches the input frequency of the generator. At resonance, amplification factors as high as 15 are obtained; these permit operation at the required g level. For higher frequencies, the force output of the generator is sufficient to drive the table at the necessary acceleration level. This concept of a "tuned" system results in a substantial cost saving when compared with the costs of purchasing the required low-frequency force in a self-contained unit.

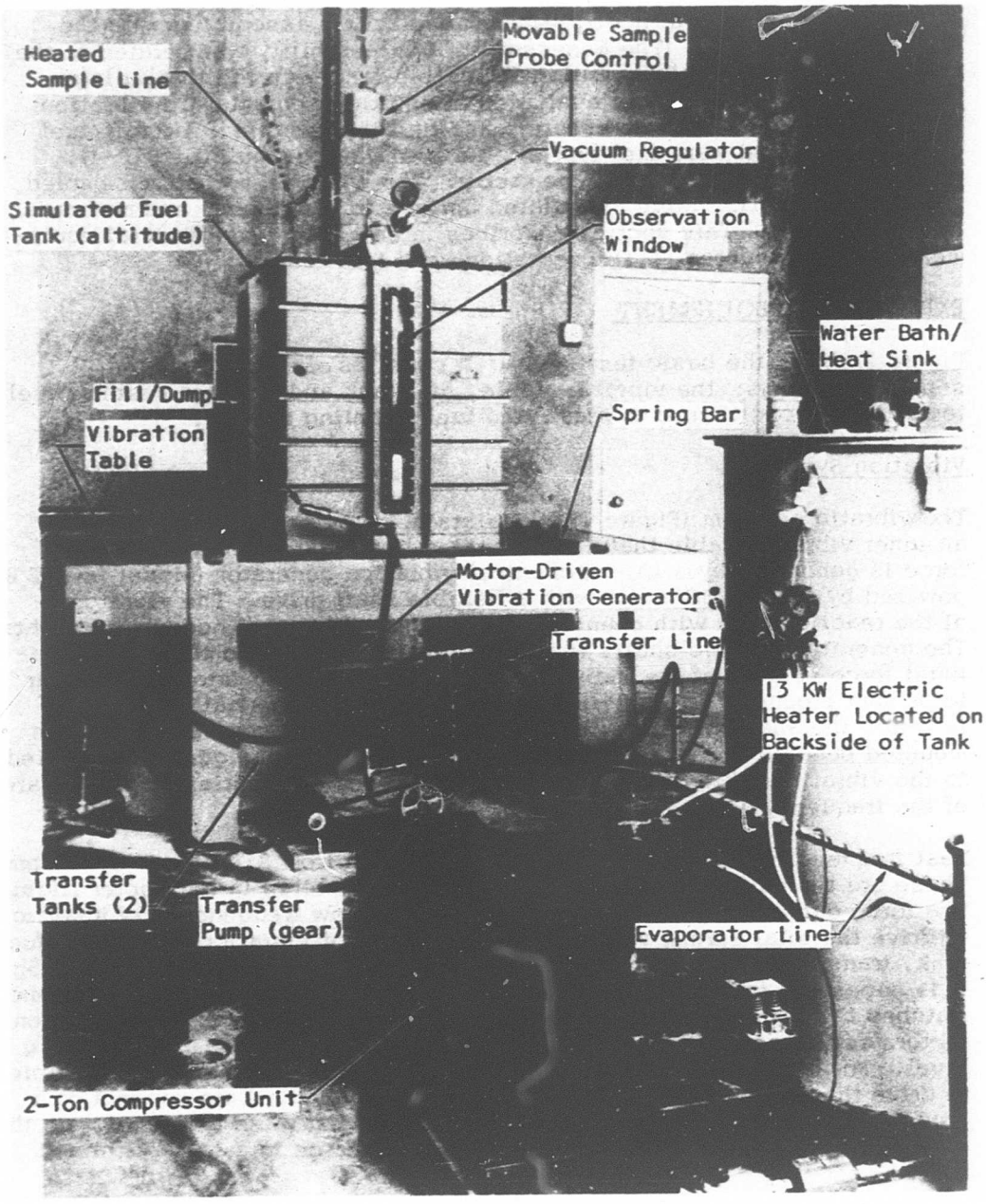

Figure 9. Test Setup.

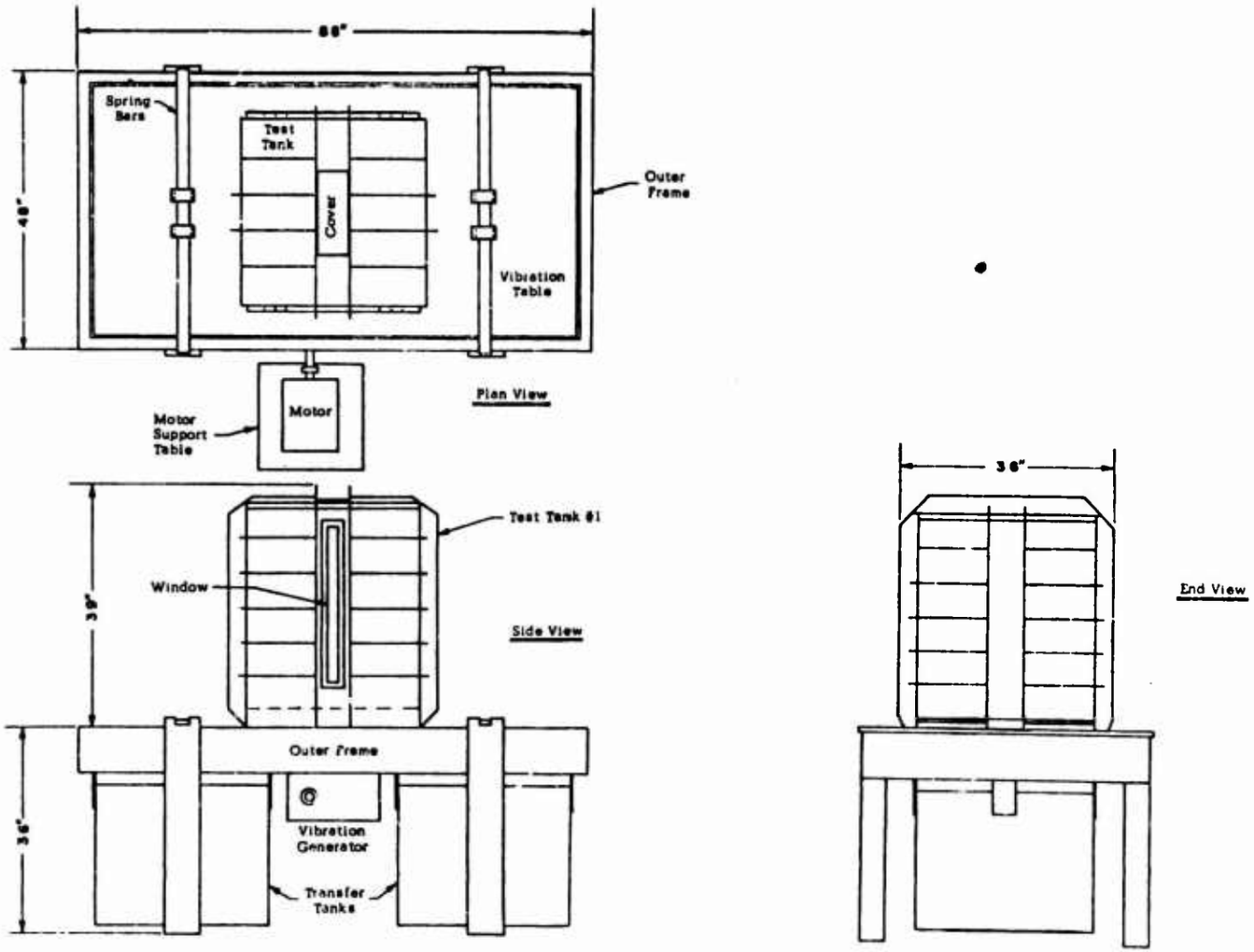

Figure 10. Overall Test Setup - Fuel Tank Vibration Test Equipment (Scale 1" = 16").

Fuel Tank and Transfer System

Three simulated helicopter fuel tank configurations were constructed (Figure 11) of 14-gauge steel tank sheet. Tank #1, which is stiffened externally for altitude, is 30 by 30 by 36 inches. It is shown mounted for test in Figure 9. The tank has longitudinal observation windows for viewing fluid motion. The top hatch is machined to accommodate the sliding vacuum joint for the movable sample probe. An air vent, to which were attached the vacuum regulator and a vacuum pump, was used to control tank pressure. Tank #2 is 18 by 36 by 12 inches. Tank #3 is cylindrical, 18 inches in diameter and 36 inches in length.

All tanks were lined (approximately halfway through the test program) with fuel cell rubber stock. This material (see Appendix II for details) is a synthetic rubber/nylon barrier material used primarily in patch-up work for fuel tank repair. It was received in a 3-foot-wide roll and was cut to fit fuel tank configurations. The liner was bonded to the metal tank wall with an adhesive. A two-day cure period is necessary for good bonding.

The experimental fuel tank (1, 2, or 3) tested was mounted on the top of the vibration table with a 1/2-inch Micarta pad for thermal insulation between the tank and the table. Beneath the vibration table were two 30-by 24-inch cylindrical fuel transfer tanks (Figure 9). These tanks are used to store fuel pumped from the experimental fuel tank to simulate engine usage (1 gpm). By maintaining this constant sprung weight, the vibration amplitude and frequency remain constant during a test.

Flexible lines and a variable-speed gear pump, used to transfer fuel from the test tank at 1 gpm, complete the fuel transfer system. This may also be seen in Figure 9. A second 20-gpm gear pump was used for filling and dumping the test fuel.

Fuel Temperature Conditioning System

The basic philosophy of the temperature conditioning system is to control the temperature of a large heat sink/water bath to the required test value. This larger thermal capacitance is then circulated through the fuel, in the case of the emulsion, or the fuel is circulated through the water bath, in the case of the liquid JP-4, until the fuel temperature reaches that of the bath. A 300-gallon tank was used to hold the water bath. A 2-ton refrigeration compressor unit was used to condition to lower than ambient temperatures. A 13-kw electrical heater mounted in the side of the tank was used to obtain higher than ambient temperature. By use of antifreeze or high-temperature fluids, it is estimated that the expected operating range of the system is from 0° to 160°F, well beyond the required test range of 40° to 100°F.

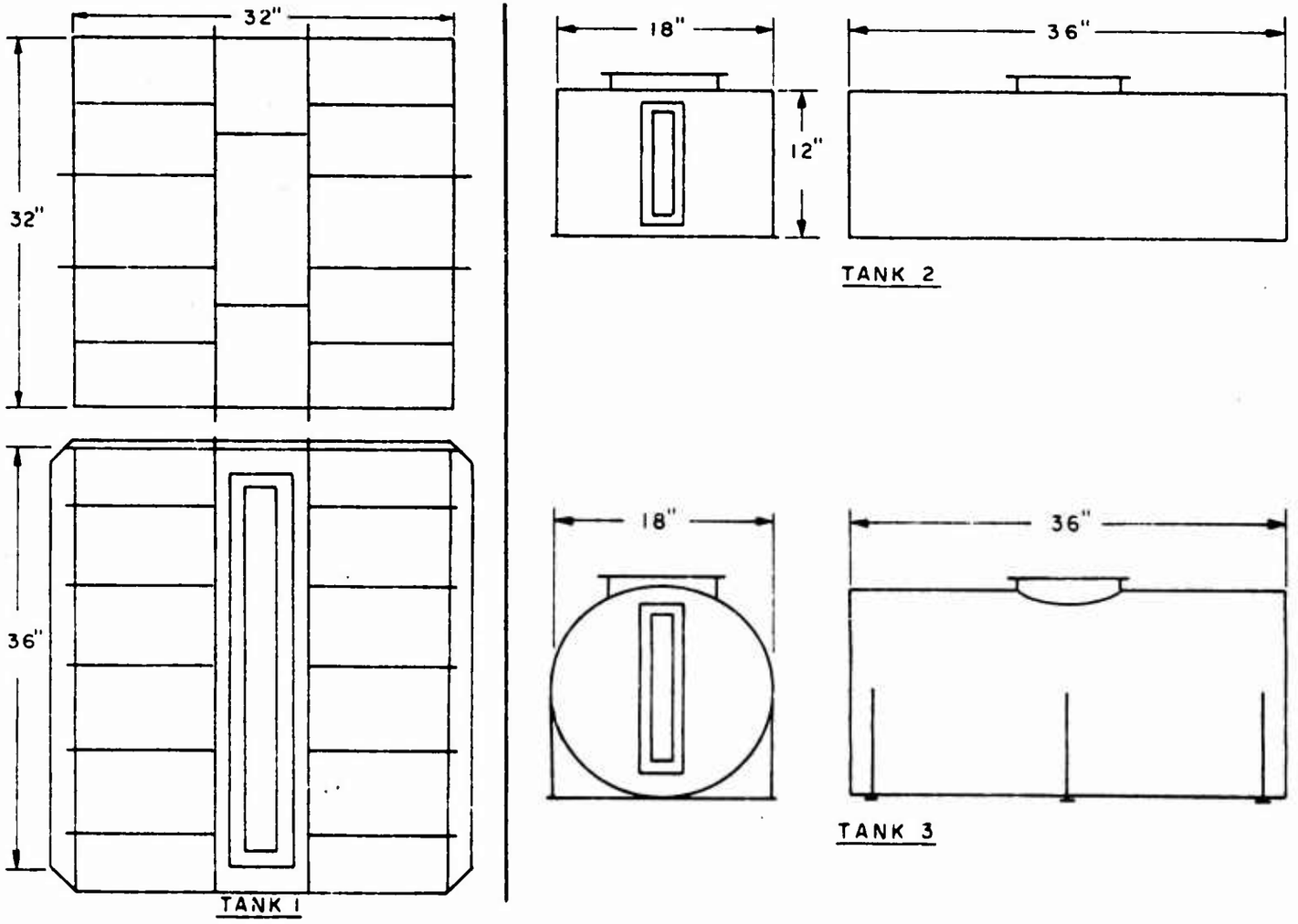

Figure 11. Experimental Fuel Tanks.

Fuel Vapor Sampling System

The experimental setup of the movable sample probe system is shown in Figure 12. The sample probe extending into the tank is 1/8-inch copper tubing. It is heated along its length to prevent sample condensation on the walls. A pulley/counterweight system is used to adjust the height of the probe in the tank throughout the test. This system is operated by one person outside the test cell and adds greatly to overall test efficiency. The sample line is enclosed in a stainless steel tube that leaves the tank through a moving vacuum seal (Figure 13). The tube provides rigidity to a tee-section. Above the weight, a flexible cable passes over pulleys and through the cell wall. The cable is counterweighted on the interior side of the wall. A pointer that is calibrated for distance into the tank is attached to the cable to permit probe depth to be read exactly off a measuring ruler mounted on the wall. The sample line passes through the wall at a location different from that of the control cable and leads to the sample input side of the chromatograph. Output is then read directly off the recorder at various depths into the tank. A mercury manometer is used to check pressure in the sample line to determine sample injection pressures. This parameter is important in the calculation of the fuel/air ratio (control sample density).

TEST INSTRUMENTATION

With the exception of the measurement of fuel/air ratio, the instrumentation employed is relatively straightforward. The basic experimental quantities being measured and the devices used are discussed below.

Fuel tank pressure (altitude) is controlled by a vacuum regulator which permits an accurate set pressure to be maintained in vacuum systems and accurately controls the amount of gas introduced. Readout is by a vacuum gauge mounted on the regulator. This gauge reads vacuum pressure accurately from 2 to 29 inches of mercury. A direct-reading mercury manometer used to measure sample pressure at the inlet of the chromatograph is used for calibration. The regulator can be seen in Figure 9.

Fuel liquid temperature is measured by a thermocouple mounted in the side of the test tank. Its calibration is confirmed during fuel temperature conditioning and filling by an immersion thermometer (done before and after test).

Vibration level and frequency are measured using two accelerometers powered by charge amplifiers. Two units were used to check for rocking by comparing phase angle between output peaks. These units were calibrated at 1 g acceleration by dropping them on a soft pad. The free-flight acceleration level is 1 g. Readout for the accelerometer and thermocouple was on an 18-channel recording oscillograph. Frequency and acceleration were then easily read by comparing output time marks and calibration displacement (1 g).

Flow rate for withdrawal from the experimental fuel test tank was measured by scaling the height change of fuel level with time and readjusting the

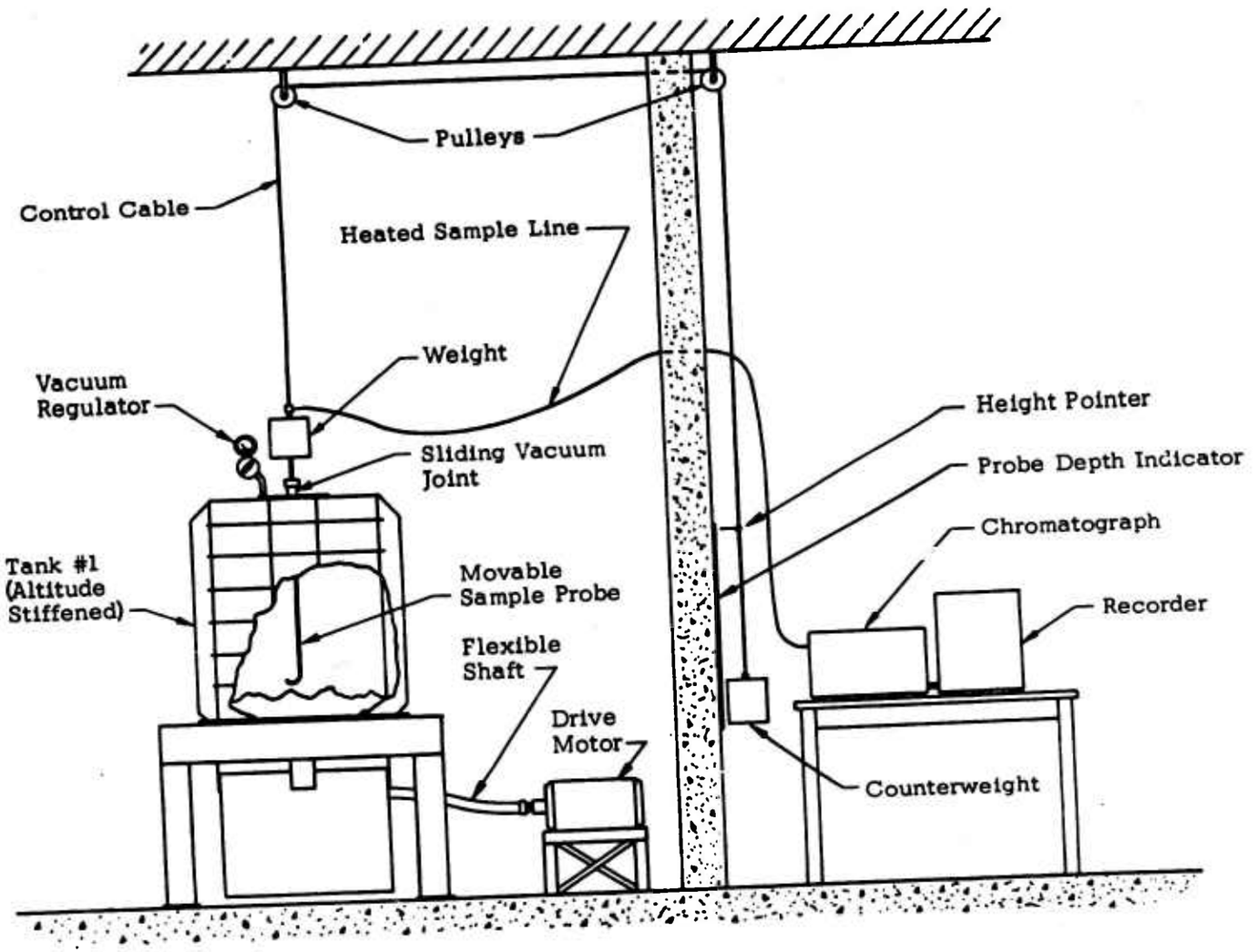

Figure 12. Movable Sample Probe System.

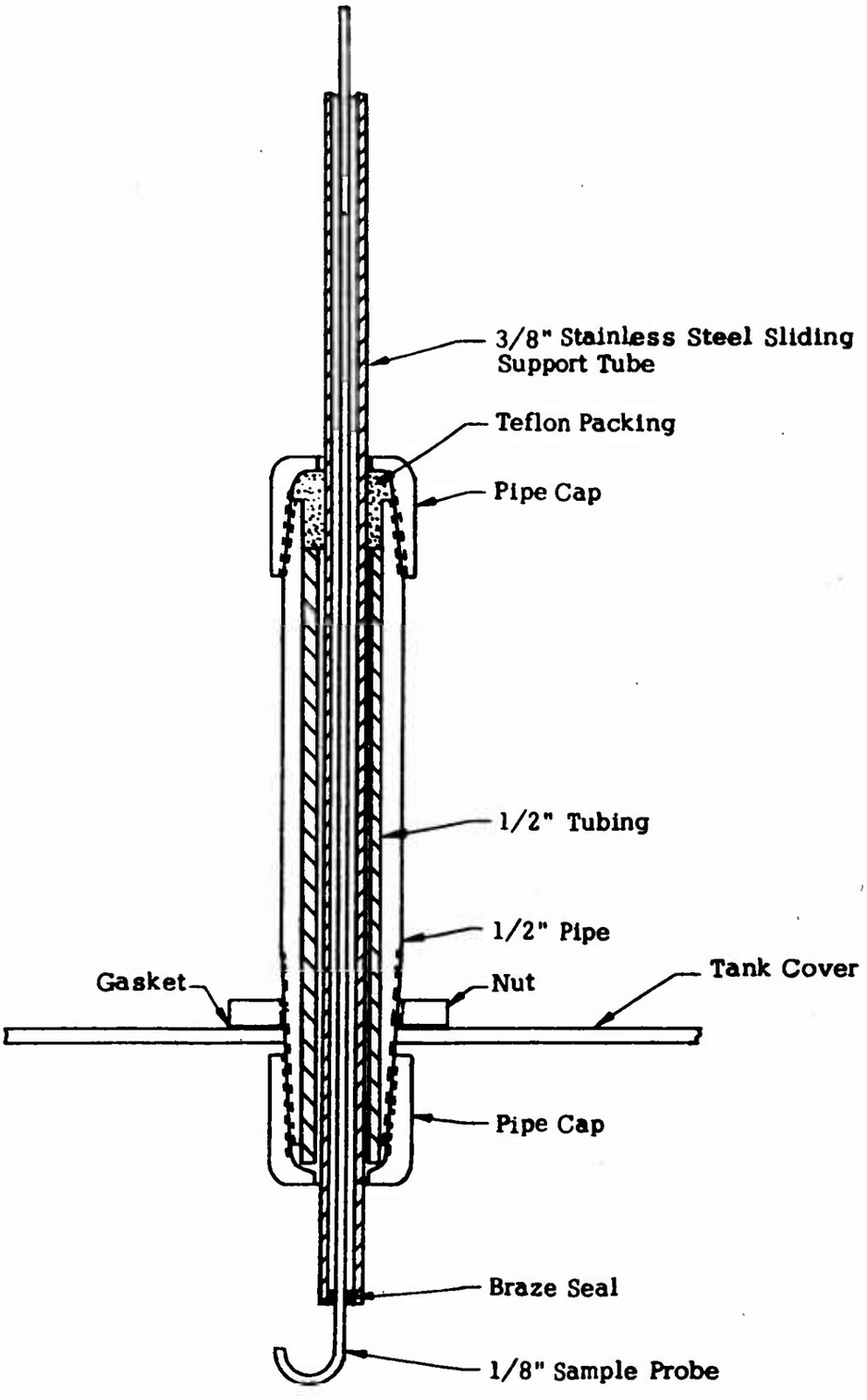

Figure 13. Sliding Vacuum Joint for Sampling Probe.

transfer pump flow rate. For Tank #1, for example, 1 gpm withdrawal corresponds to 1/4 inch per minute fuel height change. Initially, flow rate was measured by a small turbine flowmeter. However, this flowmeter was discarded as this device will not work with the emulsion.

There were several important criteria involved in choosing an appropriate instrument from which the fuel/air ratio of the vapor phase could be obtained. These include accuracy, wide composition range, variable total sample pressure, rapid sampling rate, small sample size, ease of analysis, time required for reduction of data, and cost. For the tests to be meaningful, a large number of vapor phase samples would be required to be analyzed. Therefore, the time required to withdraw and analyze the sample must be minimized without compromising the accuracy. Also because of the large number of samples, it would be desirable to withdraw very small samples so that the ullage would experience a minimum of disturbance due to removal of part of the vapor. Another major consideration was the wide range of fuel/air ratios and total pressure that would be expected during the course of testing. Many analytical instruments are effective only in restricted ranges of these variables.

A portable gas chromatograph with flame ionization detector was chosen to meet these requirements. The unit is equipped with two columns and a switching valve. The first column does not separate the sample and yields total hydrocarbon count directly. It was used to increase the speed of the fuel/air ratio measurements. The second column separates components and was used to analyze mixture hydrocarbon components to determine effective molecular weight.

It is believed that a good compromise of these varied requirements is achieved with the flow sampling system and analysis instrument shown in Figure 14. The sample is drawn through the sampling tube by a vacuum pump at a rate monitored on a small flowmeter and at a pressure monitored by a mercury manometer. The rate is such that the pressure drop in the line between the test tank and the analytical instrument is negligible, but it is also fast enough so that the total flush-out time of the sampling tube is less than 10 seconds. The sample is drawn continuously through a two-loop, manually operated sampling valve, so that a sample is injected into the helium carrier flow and analyzed by the instrument about every 30 seconds. While analysis of this sample is occurring, a new data point is being acquired by moving the sampling probe to a new position. The output of the chromatograph is in millivolts, which is a measure of the number of carbon atoms present in the sample. Procedures for calculating fuel/air ratios are shown in the following secion. This signal is recorded on a millivolt recorder having an automatic integrating circuit. The area under the millivolt versus time curve represents a quantitative measure of the hydrocarbon present in a sample. The total pressure of the sample is also measured, and these measurements, along with the calibration results, are used to determine the fuel/air ratio.

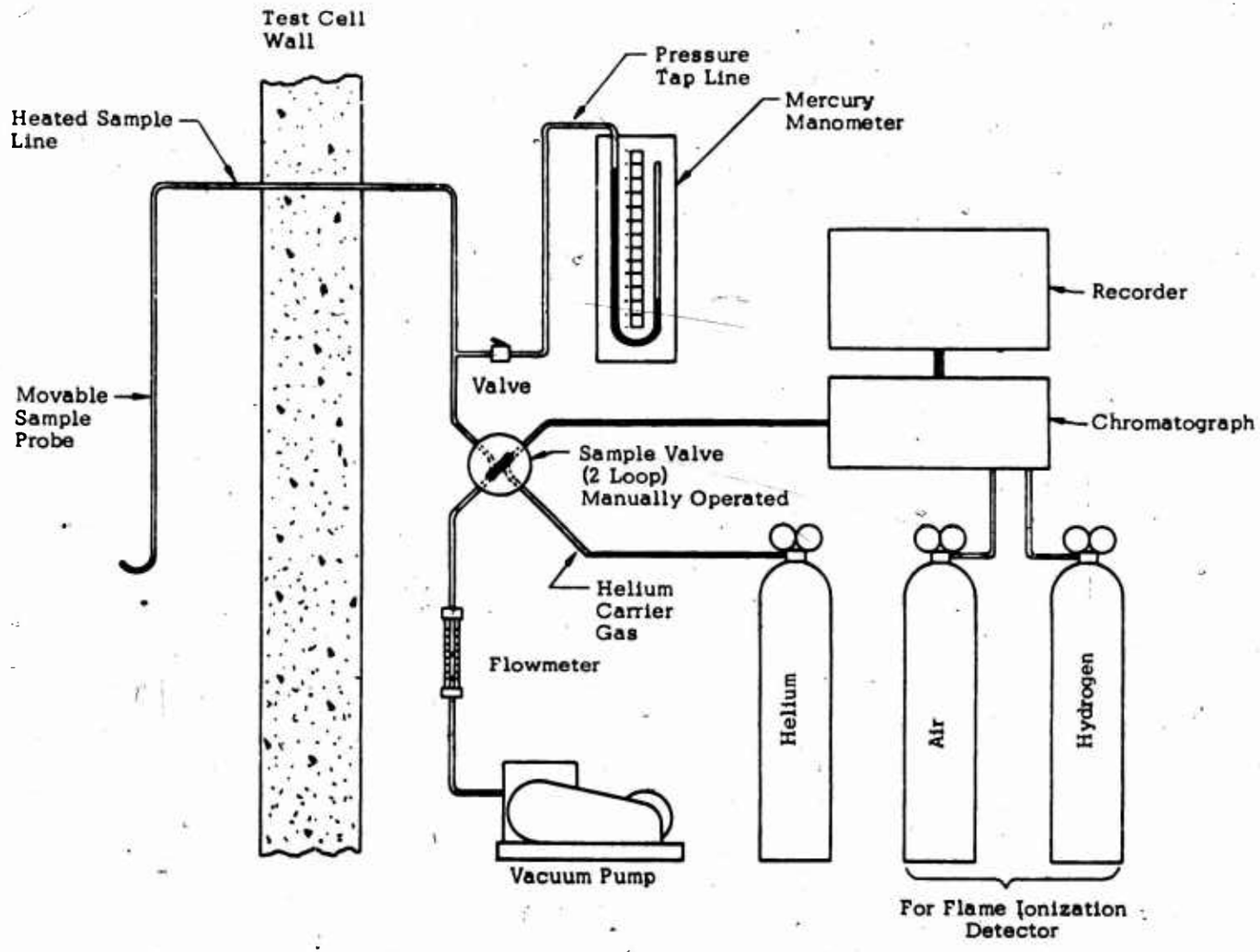

Figure 14. Flow Schematic of Sampling System.

PROCEDURES

The basic test procedure is to map the fuel/air ratio distribution as a function of position and time within an experimental fuel tank. Level-flight profiles at constant fuel temperature are flown with the fuel tank vibrated at levels resembling those encountered in actual flight. Fuel is withdrawn from the tank to simulate engine usage. The test parameters are then fuel temperature, ambient pressure, agitation, fuel type (liquid JP-4 or emulsified JP-4), and tank geometry. An additional parameter discovered during the course of testing is the exposure time of the fuel to the rubber lining material.

Prescribing a value for each of the above parameters defines a test. Following this, the initial test procedure is to condition the fuel and fill the test tank. Figure 15 shows the conditioning procedures used for the liquid and emulsified JP-4 fuels. The procedure is to control the bath temperature to the test value. For the liquid, the fuel is pumped from the drum through a heat exchange coil into the tank, using a 20-gpm gear pump. The coil is of sufficient length so that the exit temperature of the fuel is the same as that of the bath. For the emulsion, the conditioned bath water is circulated through the open-head drum of the emulsion until the required temperature is reached. The fuel is then hand-bucketed into the test tank. Hand transfer is used as the gear pump works the emulsion to a different yield stress than that at which it was received.

The chromatograph is calibrated concurrent with the fuel filling, using a standard butane air mixture obtained from a certified laboratory. These signals provide the ratio to scale from known composition to test values. Following the calibration and filling of the tank, the tank cover is replaced, if necessary, and the sample line is reconnected to the probe. The fuel temperature is recorded, and initial fuel/air mixture data are taken. The vibration generator is then turned on and adjusted until the required level is reached. Several more data points are taken to assure that the initial mixture was an equilbrium mixture corresponding to the vapor pressure of the fuel.

After the vibration level (read off the oscillograph) and the fuel/air ratio reach the prescribed test conditions, the tank pressure is set to the required value using the vacuum pump and regulator. The test is then initiated by simultaneously switching on the fuel transfer (withdrawal) pump and a timer.

The fuel/air ratio is analyzed every 15 minutes (3-3/4-inch level drop at 1 gpm) at 3-inch intervals from the top of the tank to as near the moving liquid surface as possible. The procedure is to set the indicator pointer at a 1-inch distance into the tank using the measuring rule mounted on the interior wall (Figure 12), wait for 30 seconds to assure that the sample line is full of sample gas from that point, inject this sample into the

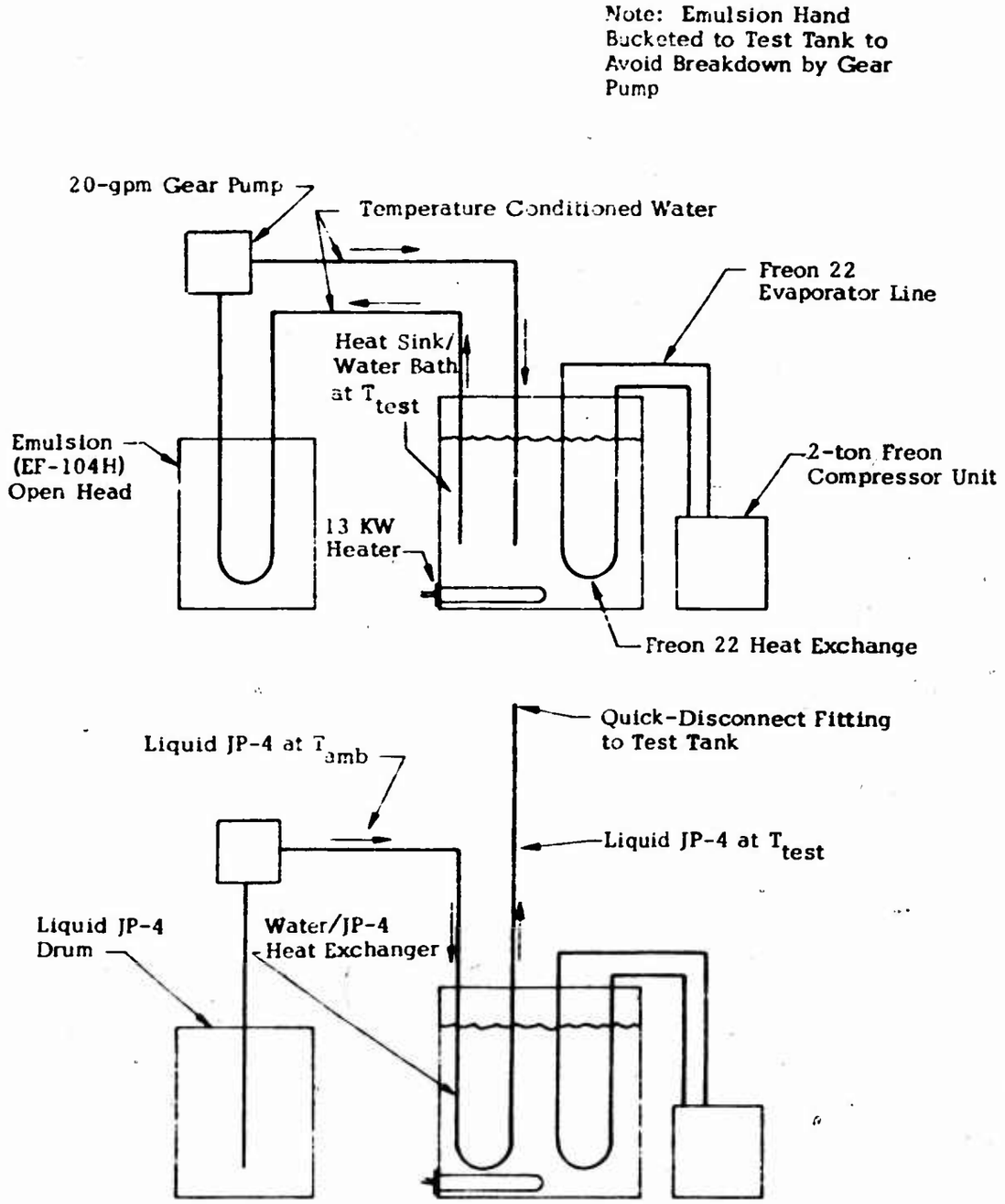

Figure 15. Fuel Temperature Conditioning Procedure.

chromatograph (analysis takes 30 seconds), and simultaneously move the pointer to the next position. This procedure is continued so that the ullage is sampled at 3-inch position intervals every 15 minutes until the tank is nearly empty. The exact time of sample injection is recorded as the surface moves between profile points. This correction for exact time of injection is small and may be neglected at the 1-gpm withdrawal rate.

The data reduction calculations used to obtain fuel pressure and fuel/air ratio are based on the use of the perfect gas law with a correction for the differences in molecular weight between calibration gas and the JP-4 mixture vapors. The flame ionization detector basically counts carbon atoms. By injecting a small sample of known fuel composition (.4% n-butane in this case) and measuring the output in terms of area under the deflection curve, the area per unit carbon atom (see Figure 16 for sample calibration and output) may be obtained. When a test sample is now measured at some point in the tank, the number of carbon atoms counted may be calculated from the ratio of the test area (A_t) to calibration area (A_c). Estimating an effective molecular weight for the complex JP-4 vapor mixture allows calculation of the moles of fuel vapor present. Moles then may easily be converted to fuel pressure and fuel/air ratio. The effective molecular weight of JP-4 based on more detailed chemical analyses using the same chromatograph was estimated to be 72 lbs/lb-mole (pentane).

These constants are combined below into two simple equations. The standard gas composition used for calibration is also built in. An additional correction for tank pressure using the equation of state is included.

$$P_f = .0461 \times \frac{A_t}{A_c} \text{ (psi)}$$

$$F/A = .00784 \times \frac{A_t}{A_c} \times \frac{P_c - .0461}{P_t - P_f}$$

where P_f = calculated vapor pressure of fuel vapors (psi)

A_t = area of chromatograph output for test sample

A_c = area of chromatograph output for calibration sample

P_c = pressure of calibration sample (psi)

P_t = pressure of test sample (psi)

The results of this data reduction program are listed in Appendix I. A simple computer program was written to perform these calculations. The input data was A_t, A_c, P_c, and P_t. The results generated were the measured vapor pressure of the fuel (P_f) and the fuel/air ratio.

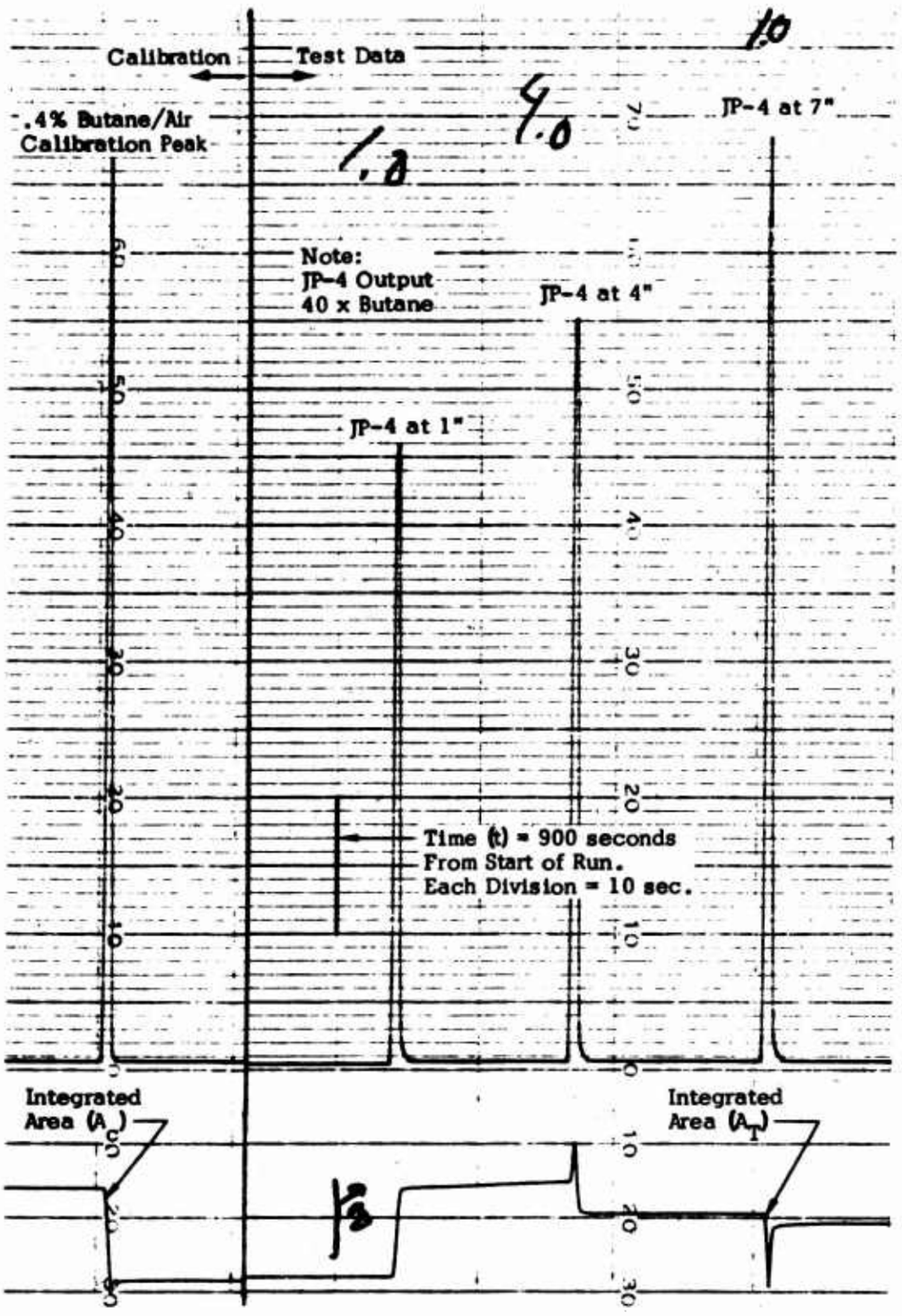

Figure 16. Sample Chromatograph Output Showing Butane Calibration and Three JP-4 Peaks at Different Positions (Test 13).

FUEL PROPERTIES

To assess the flammability characteristics of a particular fuel, the most fundamental property required is the vapor pressure. For most hydrocarbon fuels, the flammability region is bounded by fuel/air ratios of 0.035 and 0.28 by weight (Reference 1). On a weight basis, these compositions are relatively constant over the wide range of hydrocarbon types available.

Most fuel specifications prescribe a minimum and maximum acceptable Reid vapor pressure. The pressure is measured at 100°F in a container with vapor/liquid volume ratio of 4. For this work, it is essential to know the vapor pressure variation over the entire required temperature range, for only with these values may a high confidence level be placed on the experimental fuel/air ratio profile. They should approach the equilibrium value close to the liquid surface, and the equilibrium air/fuel ratio is a function of temperature and pressure.

Standard correlations exist for predicting true vapor pressure curves as a function of liquid temperature. The Reid vapor pressure at vapor/liquid volume ratio of 4 must be corrected to a ratio of zero for true vapor pressure. True vapor pressures are slightly higher than Reid vapor pressures and are easily calculated (Reference 4). The equation requires the slope of the ASTM distillation curve at the 2-percent evaporated point. For this reason, Reid vapor pressure and a complete distillation curve for the JP-4 and emulsified JP-4 (EF4-104H) were run. These results are shown in Figure 17 with calculated vapor pressure curves. From the distillation curves, it is seen that initially the fuels are quite different until the water and light ends are distilled. At the higher end they approach each other as would be expected. Also shown in Figure 17 is a special Reid vapor run taken at 40°F for the liquid JP-4 (p_v=0.5 psi).

These calculated curves derived from experimental correlations are not precise, but the important point is that they indicate that the JP-4 used was of lower than average vapor pressure. The experimental results do tend to indicate this trend.

TEST RESULTS

A summary of the different parameters used in the different tests is provided in Table I, and the results of the reduction of the experimental data are presented in Appendix II. The results are shown both in tabular and in graphical form. In the tables, time increases downward in increments of .25 hour and distance increases across in increments of 3 inches as measured from the top of the fuel tank. The results for both the partial pressure of the fuel and the fuel/air ratio are given. In the figures, concentration is specified in terms of the fuel/air ratio and the distance as measured from the top of the fuel tank. Eighteen tests are reported, and fifteen additional tests were conducted but not reported because of potential unreliability of test results. A large number of these deletions were

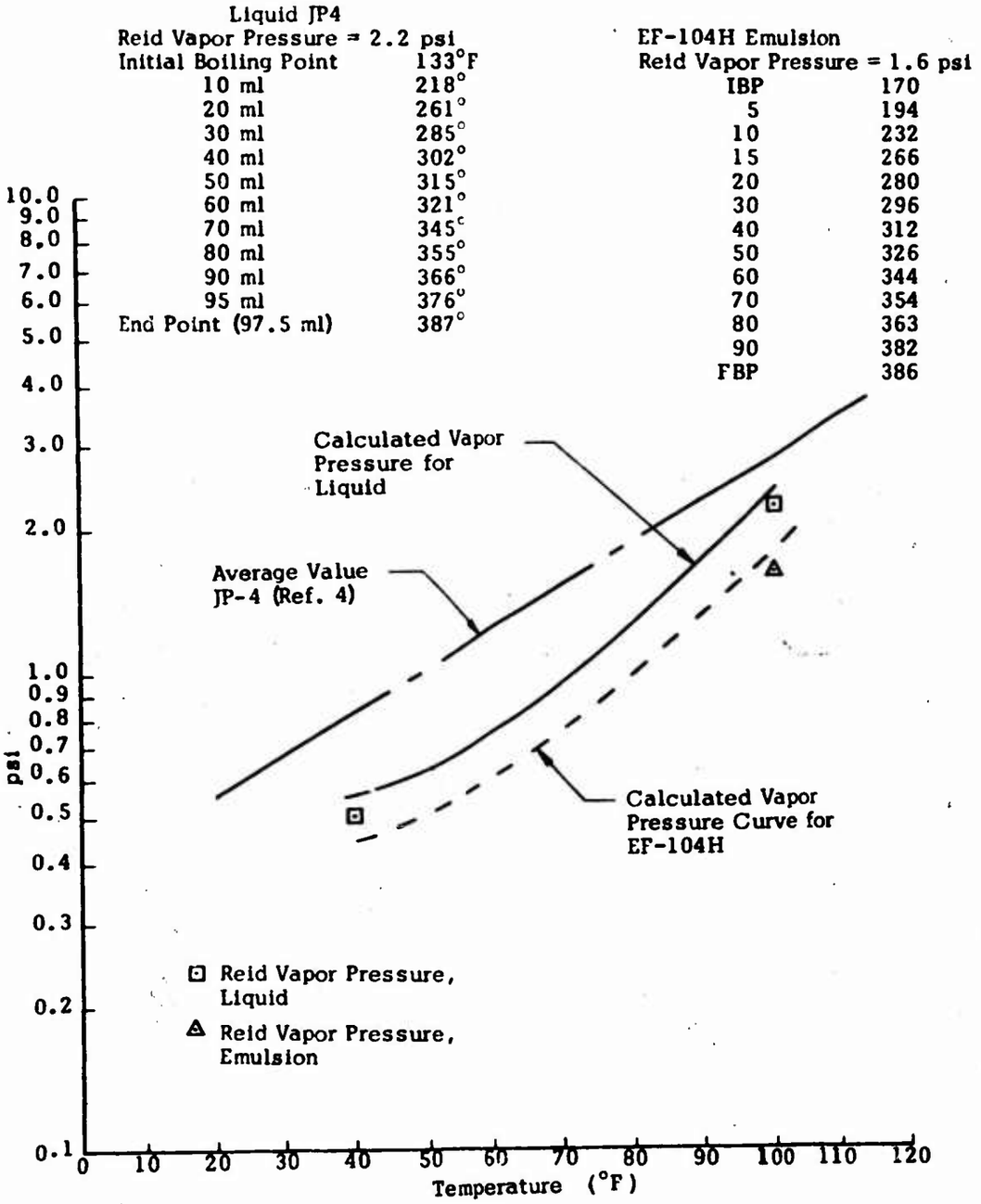

Figure 17. True Vapor Pressure of JP-4 Fuels.

TABLE I. TEST PARAMETERS

Test	Fuel	Vibration	Liquid Temp. °F	Altitude	Liner
4	Liquid	0.15 @ 5 cps	60	Sea Level	No
5	Liquid	0.15 @ 5 cps	49	Sea Level	No
6	Liquid	0.15 @ 5 cps	107	Sea Level	No
7	Liquid	0.15 @ 5 cps	52	15,000 ft	No
8	Liquid	0.15 @ 5 cps	50	10,000 ft	No
9	Emulsion	0.15 @ 5 cps	50	Sea Level	No
10	Emulsion	0.15 @ 5 cps	52	5,000 ft	No
11	Liquid	None	62	Sea Level	Yes
12	Liquid	None	48	Sea Level	Yes
13	Liquid	0.15 @ 10 cps	66	Sea Level	Yes
14	Liquid	0.15 @ 5 cps	90	Sea Level	Yes
16	Liquid	0.15 @ 5 cps	80	Sea Level	Yes
18	Liquid	0.15 @ 5 cps	46	Sea Level	Yes
19	Liquid	0.15 @ 5 cps	50	Sea Level	Yes
20	Liquid	0.15 @ 5 cps	58	Sea Level	Yes
21A	Liquid	0.15 @ 5 cps	96	Sea Level	Yes
22A	Liquid	0.15 @ 5 cps	80	Sea Level	Yes
23	Liquid	0.15 @ 5 cps	75	Sea Level	Yes

short tests to determine if the liner was saturated; i.e., a limited number of data points were taken to see whether or not a gradient was established. After some evaluation of the reliability of the test data, the results are described below in sections labeled according to the test parameter involved.

Reliability of Test Data

Some accuracy of analysis was sacrificed in order to be able to take and analyze a large number of samples. It was believed, however, that this approach would be more informative than taking fewer samples and analyzing them precisely. The large number of samples that were taken and analyzed in each test did permit a realistic mapping of the concentration profiles of the ullage as a function of time. From these concentration profiles, it was possible to deduce the effect of the various test parameters on fuel/air gradients.

There is some scatter in the data, and this seems to be more apparent in the high-temperature (high fuel/air ratio) tests than in the low-temperature tests. This might be expected, as condensation of portions of the sample (hydrocarbon loss from the sample) would be a more important consideration at high fuel/air ratios. Although the sampling line was heated well above the liquid temperature, there could have been cold spots in the sampling line system which would have caused fuel condensation. Other possible sources of error could be the inclusion of spray droplets or mist particles within the vapor sample. However, this is not believed to have been a major problem in the tests. Although surface wave motion (for JP-4) within the fuel tank was as much as 3 to 4 inches, very little foaming was produced, and only a small amount of drop formation (visual observation) was apparent. This drop formation seemed to be restricted to within several inches of the fuel surface. Spray and drop formation of a size smaller than that observable with the naked eye may have been present, but large irregularities in the composition profile which might be expected from this did not occur.

The presence of misting was not visually apparent within the fuel tank. Misting had been reported (Reference 1) previously as having a tendency to form during the ascent phase of the flight profile to an extent somewhat proportional to the rate of ascent. The current tests included only level-flight profiles; thus a comparison in this respect is not altogether valid. Turbulent eddies set up within the vapor phase by the oscillating fuel surface could cause some random fluctuations in the measured fuel/air ratio. Also, condensation of fuel vapors on the tip of the sampling probe could be a problem. An attempt was made to minimize the effect of some of these potential sources of error, but it is not known how much any of them contributed to the final result. The consistency and reasonableness of the data are the only criteria for evaluating the various effects, and considering this, there do not appear to be any important deviations.

The other variable reported is the position of the sampling probe prescribed as a distance from the top of the fuel tank. This is easily measured. However, some uncertainty is involved in locating the height of the fuel surface relative to this probe. As the fuel surface was generally in a state of high agitation, the mean height level of the liquid surface is probably not known to an accuracy greater than 1-2 inches. Therefore, the location of the fuel surface as indicated in the figures of Appendix I is somewhat arbitrary.

Fuel Temperature

Tests were conducted for fuel temperatures ranging from 46° to 107°F. The composition profiles for three of these tests (Tests 4, 6, 18) where no other parameter is being varied are shown for comparison. The fuel temperatures were 60°F for Test 4, 107°F for Test 6, and 46°F for Test 18. Although all of the composition profiles shown for these tests are relevant, the features which distinguish one test from another are most apparent in the composition profiles measured for a test time of 1.5 hours. These profiles are compared in Figure 18 and show the trends of both the magnitude and the shape of the composition profiles as the temperature of the liquid fuel increases. In Test 18 (46°F), the fuel is the coolest; this fact is reflected in the lower position of the curve on the figure. The profile drops off gradually and steadily as the top of the tank is approached. Test 4 was for a somewhat higher temperature (60°F), and the position of this profile is intermediate on the figure. A slight plateau is evident near the surface of the liquid, but otherwise the profile also drops off steadily toward the top of the fuel tank. For Test 6, an exaggerated composition plateau extends for over half of the distance from the liquid surface to the top of the tank. The dotted line shows the results of profile calculations for 1.5 hours as presented in Figures 5 through 7. For the case where the greatest agreement would be expected, Test 18 (low temperature and the assumption of $v_t/v_f >> 1$ would be best), there is some deviation. This deviation would be expected if the mechanism of transport of the fuel vapors involved some free convection or turbulence. The results of Test 4 show better agreement; it is presumed that this is so because v_f is now becoming larger because of an increase in fuel temperature, and as this happens, a composition plateau will start to develop. For Test 6(107°F), the composition plateau has developed significantly.

The results were repeatable with the exception of Test 5 (50°F). In this test, the composition dropped off from the value at the fuel surface and then remained level through the remainder of the ullage. This type of profile was not expected, Errors could have been introduced during some of the experimental procedures, but as there was no reasonable cause for deleting these data, they have been included. However, the results of the other tests in this temperature range are sufficiently consistent, so the discrepancy of Test 5 is not considered to be serious.

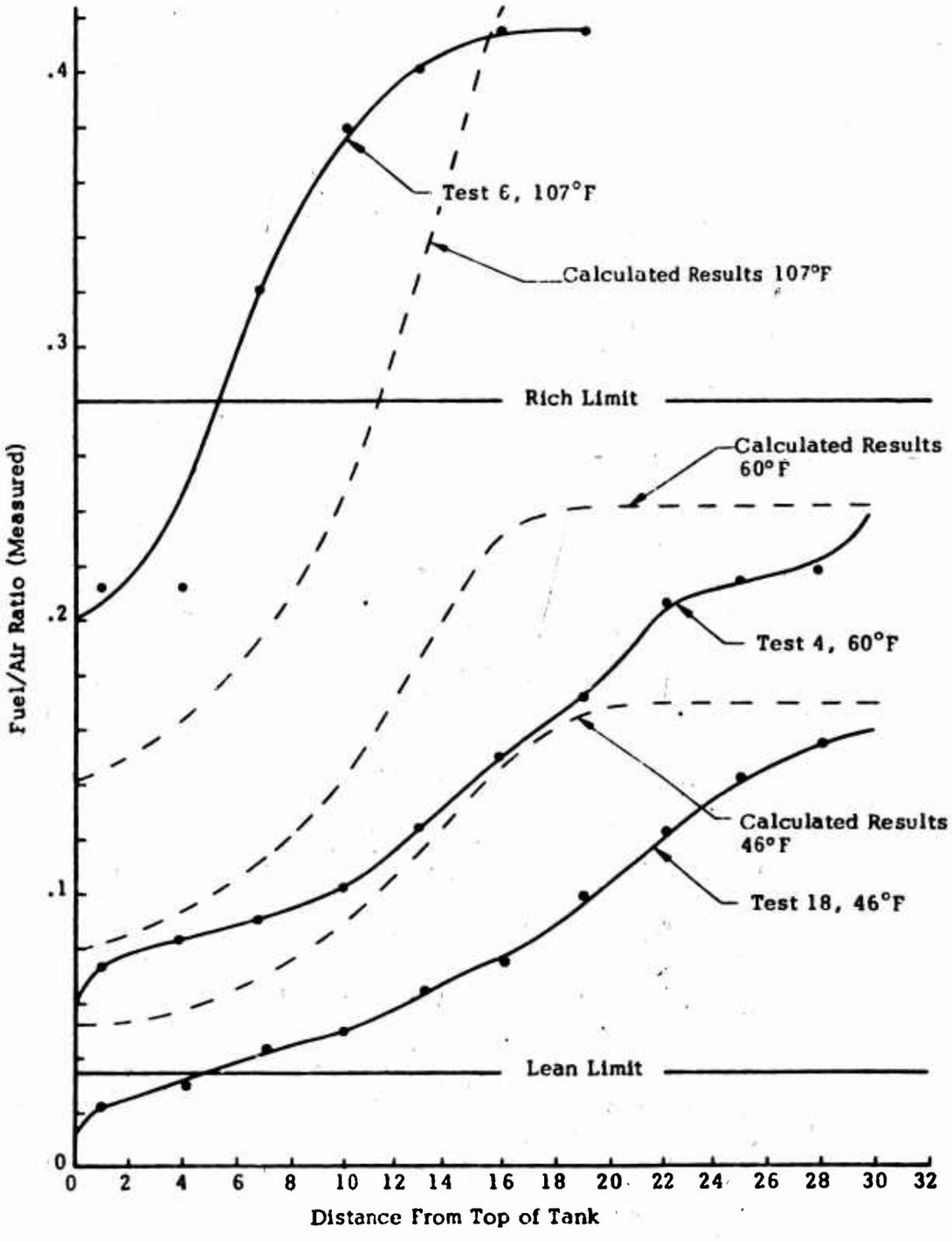

Figure 18. Empty Tank Fuel/Air Composition Profile at Various Fuel Temperatures (Sea Level).

Altitude (Test Pressure)

The effect of ambient pressure on the composition profiles is shown in the results of Tests 19, 8, and 7 (50°F), which were conducted at simulated altitudes of sea level, 10,000 feet, and 15,000 feet respectively. The results of Test 19 are typical of these tests conducted at a relatively low temperature and atmospheric pressure. In Test 8 (10,000 feet), the shape of the composition profiles has started to level off; in Test 7 (15,000 feet), the composition profile is level. As test pressure decreases, the fuel/air ratio at constant fuel temperature increases. Figure 19 compares the results of these tests for a test time of 1.5 hours. In this case, two factors are contributing to the flatter profile. First, by decreasing the total pressure within the fuel tank, the percentage of fuel vapor in the ullage doubles. This increases the bulk fluid motion in the vapor space (v_f) due to fuel evaporation. A second factor is that the solubility of air within the liquid decreases in direct proportion to the ambient pressure (Henry's Law). As the ambient pressure decreases, air that was soluble for an applied pressure of 1 atmosphere now reaches a state of supersaturation, and it starts to evolve from the liquid phase in the form of bubbles. As these bubbles pass from the surface of the liquid, they carry with them an equilibrium concentration of fuel vapors. This deaeration is another contributing factor to the bulk velocity coming from the surface (v_f).

Vibration of Fuel Tank

The effect of fuel tank vibration on transport of fuel vapors from the liquid to the gas phase and then through the gas phase to the top of the tank was measured at two temperatures. This is shown at 48°F by Tests 18, 12, and 19 and at 62°F by Tests 4, 11, and 13. Composition profiles for a test time of 1.5 hours for these two temperatures are compared in Figures 20 and 21. Figure 20 compares results for Tests 18 and 19 where the fuel tank is subjected to a nominal vibration (5 cps @ .15 g maximum acceleration) and for Test 12 where no vibration is imposed. Figure 21 shows results for Test 11, which is not subjected to any vibration; Test 4, which is subjected to the nominal vibration; Test 13, where the frequency of vibration has been changed (10 cps, .15 g maximum acceleration).

No differences in the composition profile are apparent. The levels of the curve are approximately the same, and the shapes are similar. The fact that the composition profiles are similar indicates that the mode of transport of the fuel vapors from the surface to the top of the ullage is probably the same for both the condition where the tank is vibrating and the condition where it is not being disturbed. Therefore, although there are modes of transport other than molecular diffusion (free convection, for example) involved, they do not appear to be related to the agitation that was imposed on the tank within the limited range of frequencies investigated. Even at the no-vibration condition (vibration generator off), a limited amount of force was transmitted to the tank by the lines attached to the transfer pump. It must be recognized that when relating these results to aircraft, no aircraft motion such as shock due to course changes and atmosphere turbulence was included in the simulation.

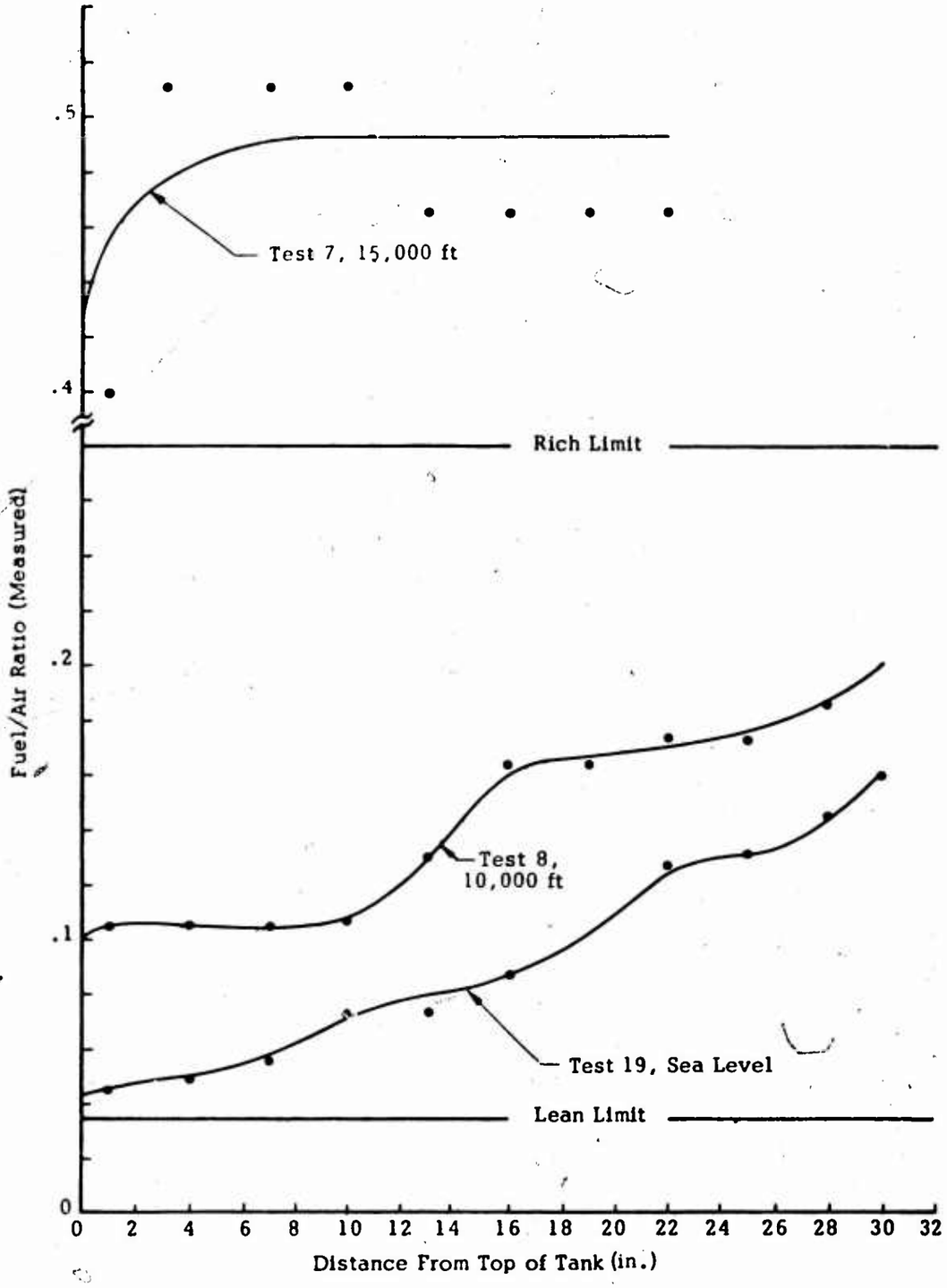

Figure 19. Empty Tank Fuel/Air Composition Profile at Various Pressures (50° F).

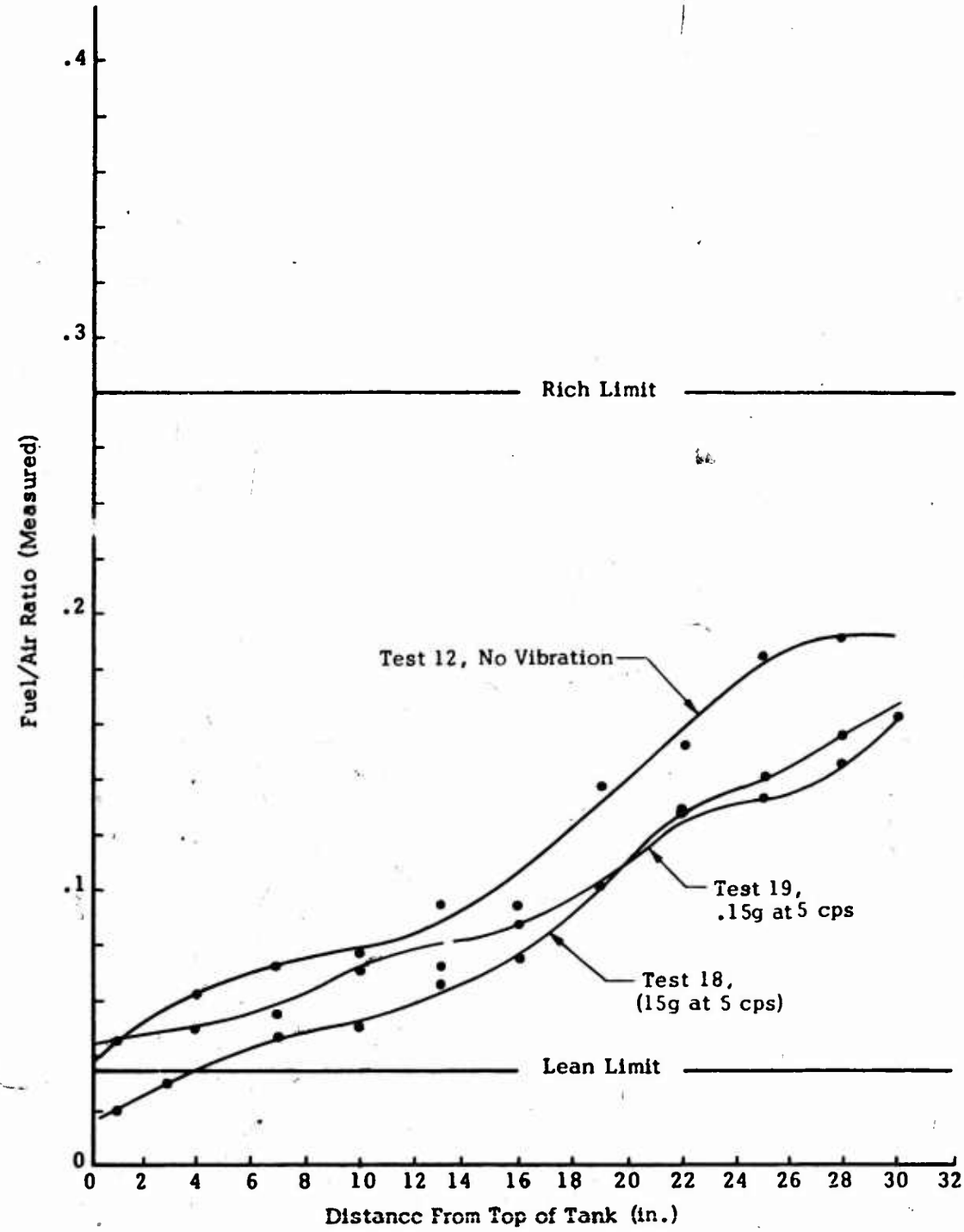

Figure 20. Empty Tank Fuel/Air Composition Profiles Showing Effect of Vibration (48°F, Sea Level).

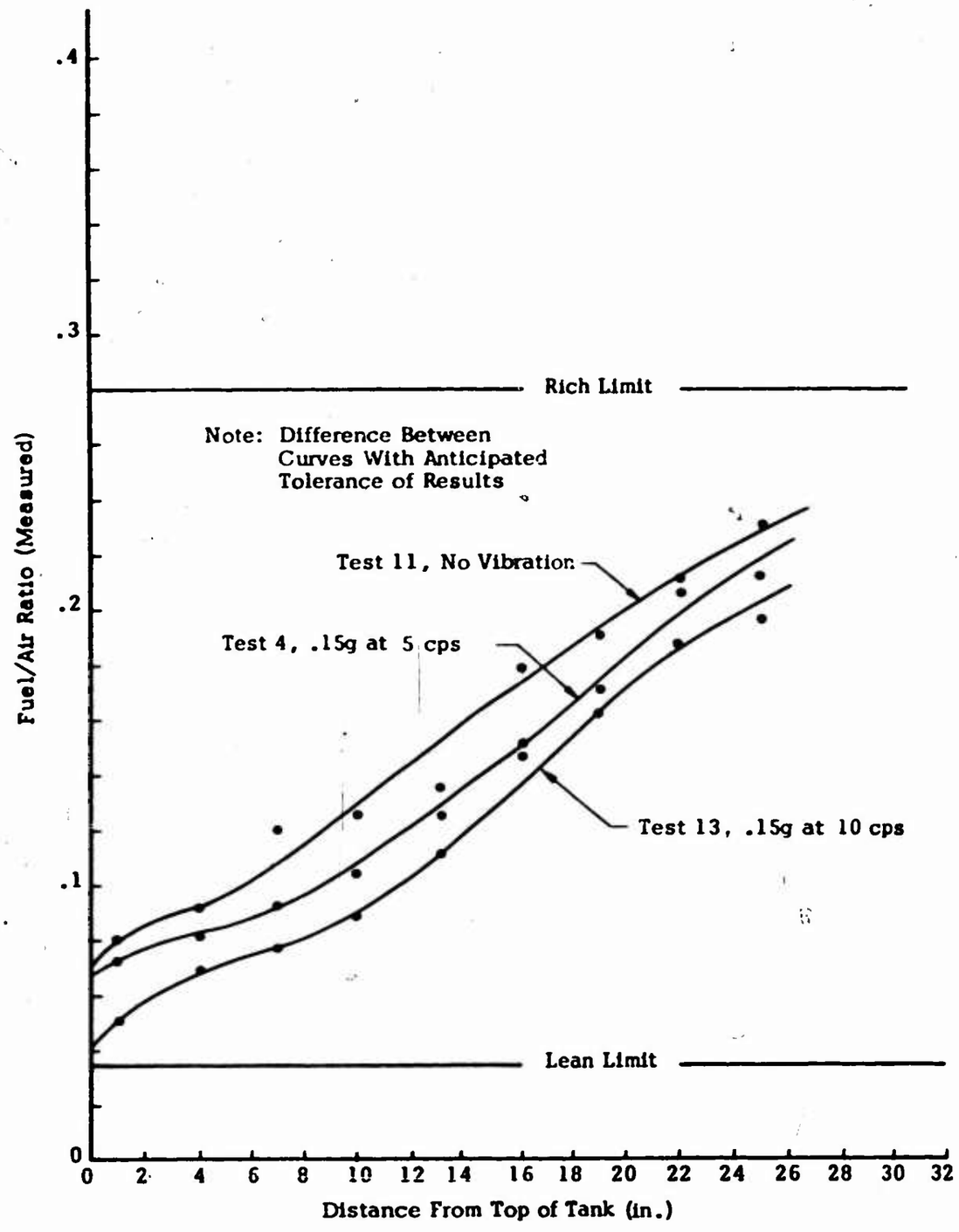

Figure 21. Empty Tank Fuel/Air Composition Profiles Showing Effect of Vibration (62° F, Sea Level).

Fuel Tank Liner Effects

Tests 4 through 10 were conducted with an unlined (interior of fuel tank exposed to metal wall) fuel tank. The fuel tank was then lined with a standard synthetic rubber tank lining material (PF-10056), and the remainder of the tests were conducted. The test results showed that differences occurred in the composition profiles which appeared to be related to the presence or absence of the fuel tank liner. These differences were not always apparent, but they seemed to be related to the history of the fuel tank liner and the temperature of the liquid fuel. The manufacturer of the rubberized lining material was contacted to obtain additional technical data on the liner, and some additional laboratory tests were conducted in this program in an attempt to evaluate these effects. These tests are explained in detail in Appendix II. In general, they showed (as was confirmed by the manufacturer of the liner) that upon exposure to JP-4 fuel, some of the plasticizing components of the liner migrated into the fuel.

This process of migration of the plasticizer out of the liner is essentially complete within several days, and once a fuel tank has been used several times, no further changes in the composition of the liner would be anticipated. As the plasticizer is removed from the liner, some of the liquid fuel components, particularly the aromatic ones, become absorbed within the matrix of the liner structure. These compounds apparently are not tightly bound to the liner material and may be driven off at moderate temperatures (75° to 80° F in this investigation). Realizing that a fuel tank may undergo many types of environmental changes, the saturation of the liner material for any particular flight would depend upon the immediate past history of the fuel tank. For example, if the fuel tank is allowed to sit full of fuel for several days, the liner will become saturated with those components of the fuel which it absorbs. Even those portions of the liner material not in direct contact with the liquid (top of the tank, for example) may absorb considerable amounts of fuel from the vapors present. Depending upon the temperature of the fuel tank walls, these fuel vapors may be driven out into the vapor space as the liquid fuel level recedes. In a particular flight profile, either a great deal or very little of the absorbed fuel components could be driven out of the liner into the ullage Thus, the condition of the liner for a succeeding flight is affected.

After the liner was initially put in the fuel tank, the tank was never completely emptied, although it did sit with varying amounts of fuel for several days at a time between tests. Therefore, the condition of the liner at the start of any given test was essentially unknown. An exception might be Tests 11 and 12, the first tests where a liner was used, where it might be assumed that the liner had not yet been saturated with fuel. It then becomes apparent that each test must be considered by itself to determine the extent to which the liner may have affected the measured composition profile within the ullage space.

Examples of the tests where the rubberized liner had a measurable effect on the composition profile were those where the fuel temperature was somewhat elevated (Tests 14, 16, 22A, and 23). In these tests the fuel temperature ranged from 75°F (in Test 23) to 90°F (in Test 14). Tests 22A and 23 (Figure 22) are characterized by a dip in the concentration profile, so that a minimum in the fuel/air ratio is observed to occur midway between the lined top of the tank and the liquid fuel surface.

At first glance, the dip would seem to be due merely to diffusion into the ullage of fuel vapors from both the top of the tank and the surface of the liquid. This is not the case, however, as it is likely that a three-dimensional mixing from all the walls is involved in causing the dip.

In contrast to the above, Tests 14 and 16 (90° and 80°F respectively, Figure 23) exhibit almost no concentration profile. It could be that the effect of the fuel tank liner is greater in these two tests, but it is also possible that motion from the surface (v_f) is contributing to the flatness of the profiles. Test 6 is an interesting comparison for an unsaturated liner case. The composition profile is level for the greater part of the distance separating the top of the ullage and the fuel surface. A rapid decline in the amount of fuel vapors present occurs as the top of the ullage is approached. In this test, the tank liner was not involved as a source of fuel vapor at the top of the tank. The comparison shows that the liner can have a significant effect on the composition profile for certain conditions of exposure time and liquid temperature.

Fuel Emulsion EF4-104H

Figure 24 presents the results of Tests 9 and 10 run with emulsified fuel. Generally, as would be assumed from the vapor pressure curve of Figure 17, the emulsified fuel results in a lower fuel/air ratio than JP-4 at corresponding conditions. The composition profile generally appears more uniform than for the liquid.

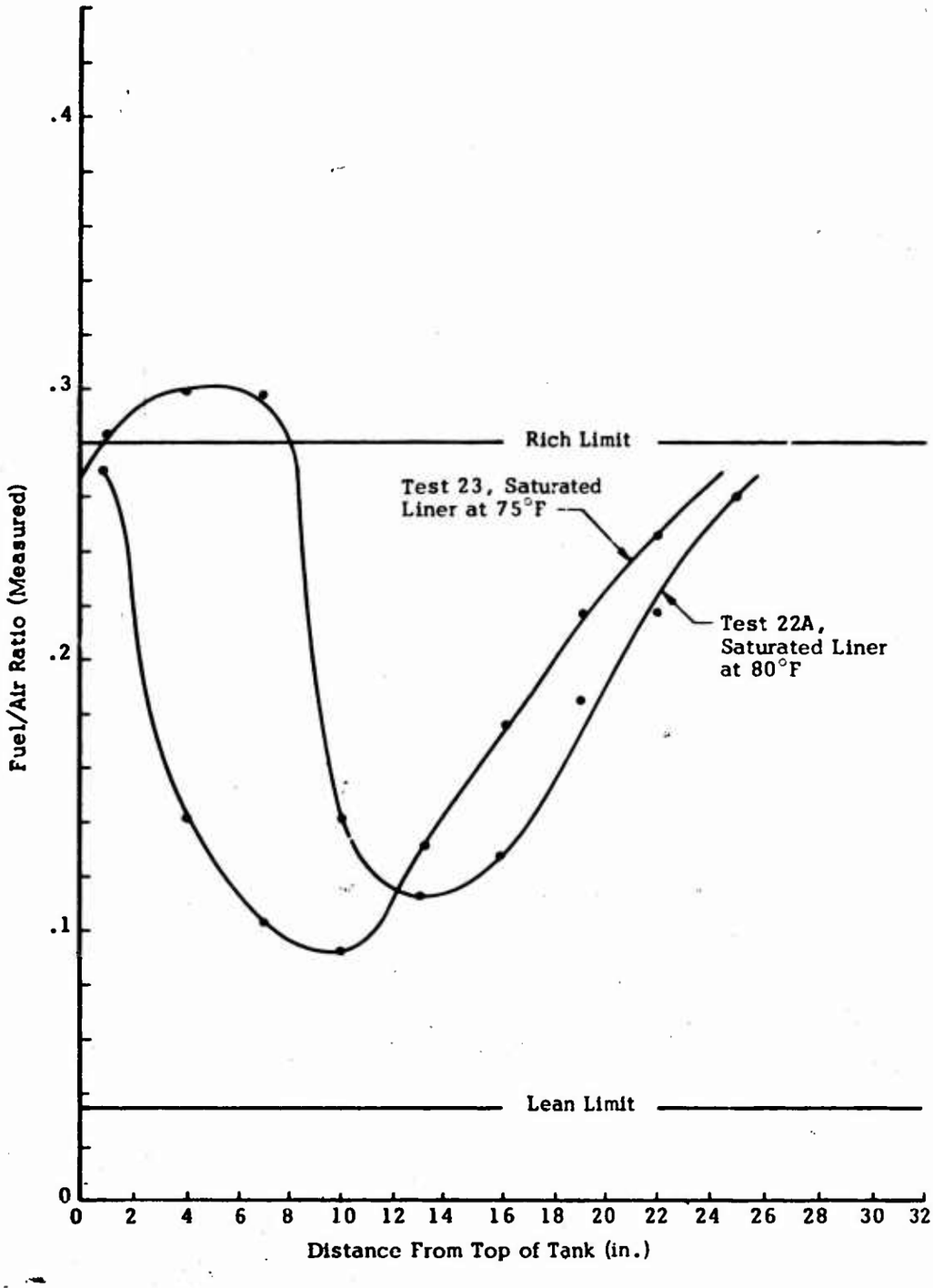

Figure 22. Empty Tank Fuel/Air Composition Profiles Showing Effect of Liner Saturation.

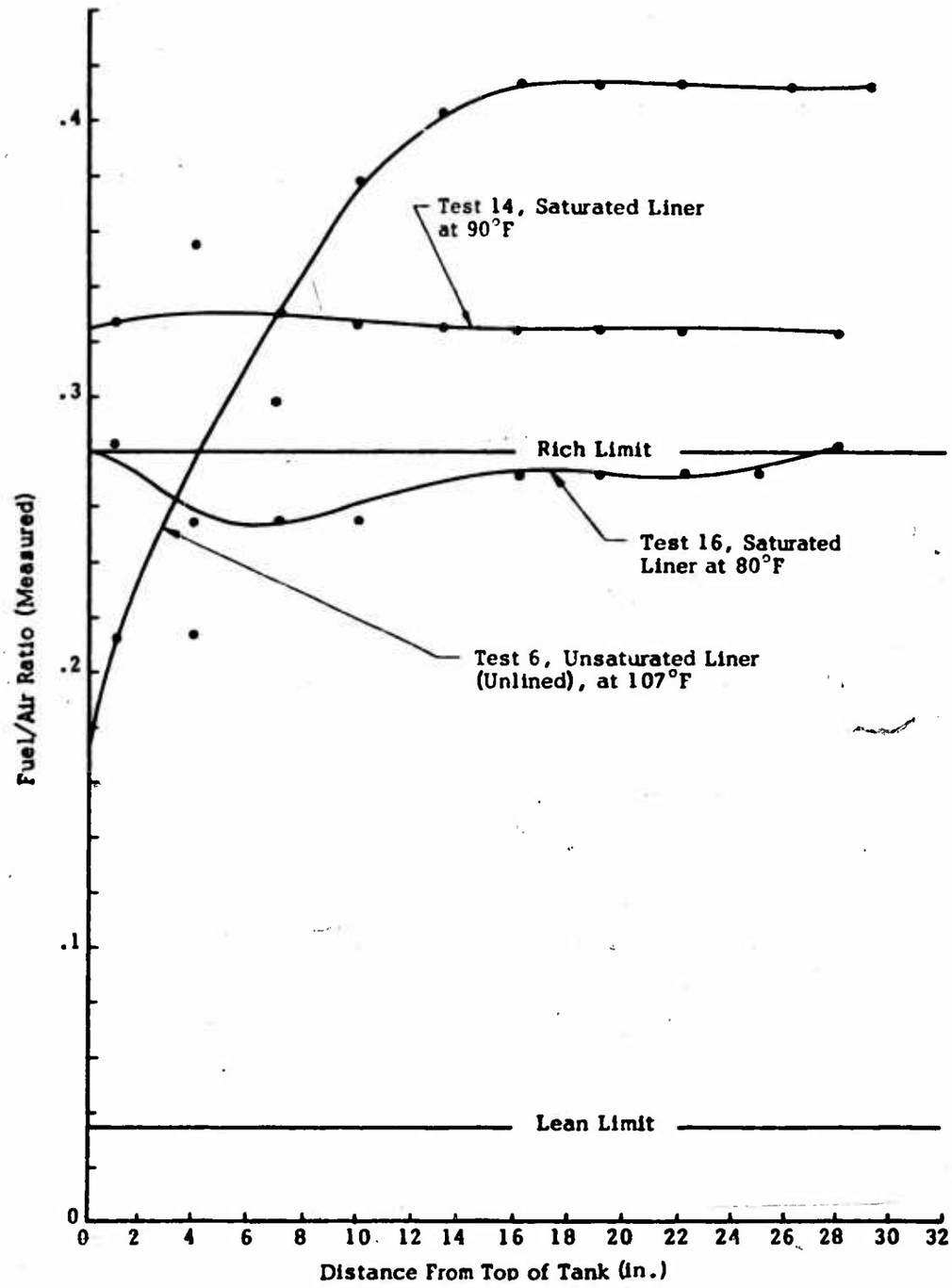

Figure 23. Empty Tank Fuel/Air Composition Profiles Showing Effect of Saturated and Unsaturated Liner.

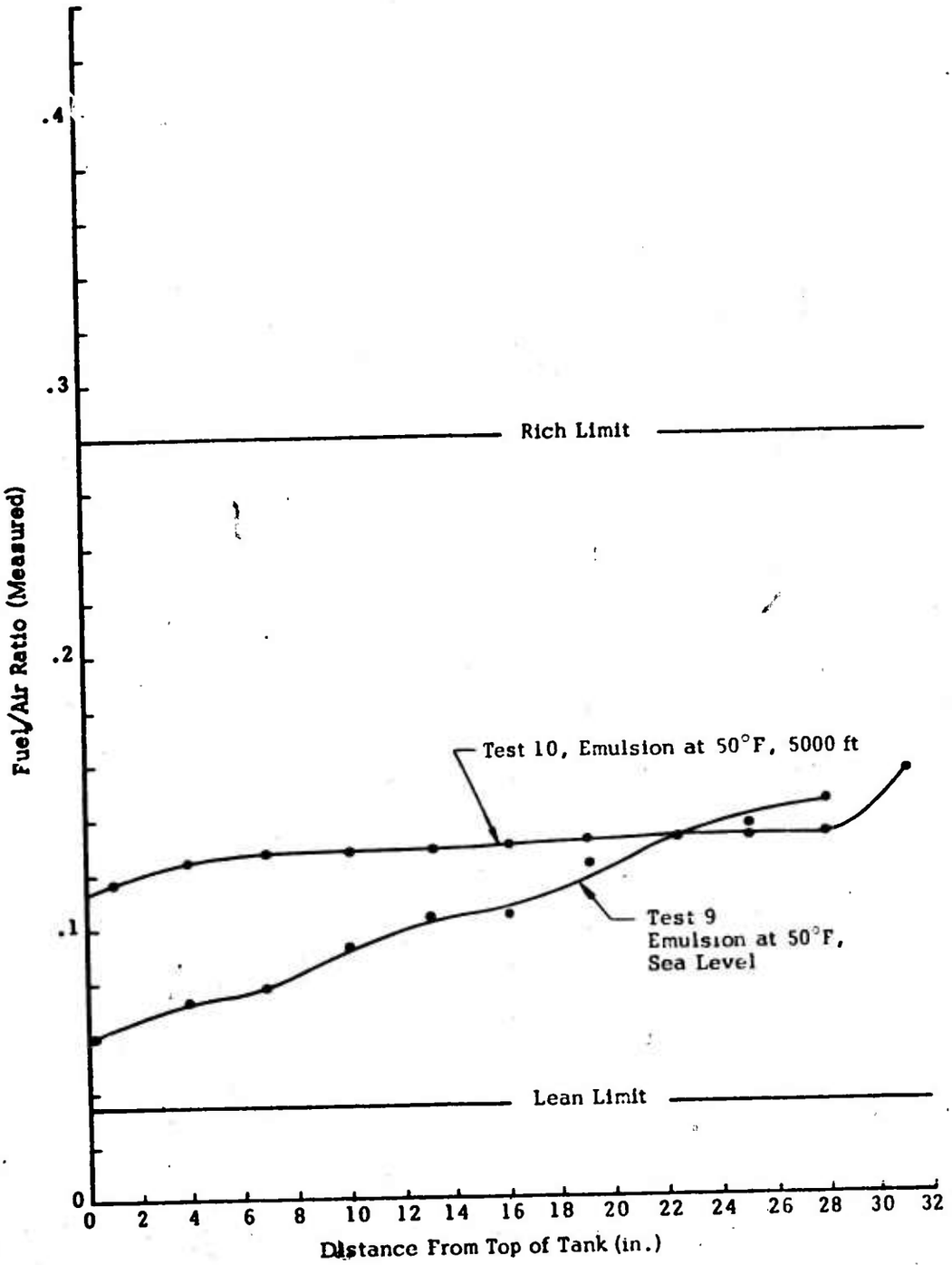

Figure 24. Empty Tank Fuel/Air Composition Profiles Showing Differences Between Emulsion (EF4-104H) and JP-4.

CONCLUSIONS

Fuel/air gradients were found to exist in the ullage space under simulated flight conditions. These results differed significantly from those which would be found if the vapor mixtures in the ullage were considered to be at equilibrium (i.e., a uniform vapor mixture with fuel partial pressure identical to the vapor pressure of the contained fuel). The gradients are such that tanks considered to be fuel-rich under equilibrium conditions do indeed contain varying amounts of flammable mixture. The effects of liquid fuel temperature, altitude, agitation of liquid, fuel type, and a fuel tank liner on the measured fuel/air ratios were determined.

1. Increasing the liquid fuel temperature (test range 40° to 100° F) increases the overall fuel/air ratio. Even at 107°F (equilibrium fuel/air well above fuel-rich limit), a portion of the ullage space was still within flammable ranges due to the existence of fuel/air gradients. Increasing the temperature also causes the near-equilibrium fuel/air mixtures to extend further out from the fuel surface. In essence, then, nonequilibrium venting effects, due to fuel withdrawal, extended the nominal flammability-rich limit (60° F in Reference 1) to over 100° F because of the fuel/air gradients.

2. At sufficiently high temperatures (75° to 80°F) in a rubber-lined tank, the wall of the tank was warmed to the extent that fuel absorbed in the liner evolved as fuel vapor. This caused a decrease in the vapor phase fuel/air gradients as compared to the unlined fuel tank. Depending on the degree of saturation of the liner, this effect can reduce the quantity of flammable vapor.

3. As altitude increased, the composition profile became flatter. This was due to the increased volatility (interphase mass transfer) of the liquid as the pressure decreased. Also, air saturated with fuel vapors evolved from the liquid solution (see Appendix III).

4. In the tests conducted, the vibration of the fuel tank at different g levels and frequencies (agitation of liquid) did not affect the composition profile. This result indicated that the controlling transport mechanisms were similar with and without vibration. Therefore the agitation of the fuel was not a significant factor. The nominal rectilinear vibration of .15g and 5 cps resulted in 3-to 4-inch waves (peak-to-peak), but very little foaming, spray, or misting occurred (Reference 1).

5. The emulsified fuel (EF4-104H) showed a lower vapor fuel/air ratio than the liquid fuel. Generally, smaller fuel/air gradients were observed with the emulsified fuel than the liquid fuel.

An analytical model to simulate the diffusion within the fuel tank and convection of the vent air was developed. The model was based on extension of an existing heat transfer program to include vent convection. Calculations made using the program compared reasonably well with experimental results.

Agreement between the experimental data and calculated results indicates that a reasonable understanding of the effects of various flight parameters on fuel/air gradients in the ullage space has been reached. The analytical model aids in predicting fuel/air gradients within aircraft fuel tanks of different geometries and for arbitrary flight profiles.

RECOMMENDATIONS

The following recommendations are made for future work to define more completely the extent of the mixture of the fuel/air gradients problem and to lead to a practical solution:

1. Conduct additional tests to cover more completely the range of flight/aircraft parameters including ascent (air evolution from liquid) and descent (high vent air convection rates) effects on vapor phase gradients.

2. Add fuel volatility convection term to tank computer model, correlate with above test results, and generate a set of calculated composition profiles for various flight profiles expected in operation. From these results, a pilot's handbook of safe flight envelopes can be generated.

3. Demonstrate the validity of the above results for several test profiles with a spark ignition explosion-proof tank. Tests can be conducted to measure and classify the intensity of ignition.

4. Based on an understanding of fuel tank transport behavior and the calculated composition profiles, indicate methods of solution and define test verification procedures.

LITERATURE CITED

1. Nestor, L. J., INVESTIGATION OF TURBINE FUEL FLAMMABILITY WITH AIRCRAFT FUEL TANKS, FAA No. DS-67-7, Naval Air Propulsion Center, Naval Base, Phil., July 1967.

2. Helgeson, N. L., et al, SUPERSONIC AIRCRAFT FUEL TANK FIRE HAZARD INVESTIGATION, Dynamic Science, AFAPL-TR-68-106, Air Force Aviation Propulsion Laboratory, December 1968.

3. Bird, Steward, Lightfoot, TRANSPORT PHENOMENA, John Wiley and Sons, Inc., New York City, 1960.

4. Barnet H. C., et al, PROPERTIES OF AIRCRAFT FUELS, NACA/ Lewis Research Center, Cleveland, O., NACA-TN-3276, Aug. 1956.

5. Bartocha, B., Graham, W.A.C., Stone F.G.A., HYBRIDE-TRANSFER REACTIONS OF BORINE, J. Inorg. Nucl. Chem. 6 pp 119, 1958.

6. Polishuk, A. T., Kennedy, R. M., and Jezl, J. L. GAS SOLUBILITY STUDIES OF JET FUELS, SAE J 67, pp 72, 1959.

TEST RESULTS - FUEL/AIR RATIO VS DISTANCE FROM TOP OF TANK

TESTNO 4 JMAX 4 ACAL 8H PCAL 14.70 PTEST 14.70

TIME/DIST		1	4	7	10	13	16	19	22	25	28
0.00	PRESF	1.363									
	F/AIR	.2545									
.25	PRESF	.870	1.122								
	F/AIR	.1567	.2058								
.50	PRESF	.765	.912	.996	1.153						
	F/AIR	.1368	.1648	.1810	.2120						
.75	PRESF	.702	.744	.828	1.090	1.101					
	F/AIR	.1256	.1329	.1487	.1995	.2016					
1.00	PRESF	.577	.650	.681	.839	.996	1.048	1.101			
	F/AIR	.1017	.1152	.1211	.1507	.1810	.1913	.2016			
1.25	PRESF	.461	.524	.598	.629	.839	.923	1.101	1.122		
	F/AIR	.0807	.0921	.1055	.1113	.1507	.1668	.2016	.2058		
1.50	PRESF	.419	.472	.524	.577	.702	.839	.943	1.122	1.153	1.174
	F/AIR	.0731	.0836	.0921	.1017	.1250	.1507	.1708	.2058	.2120	.2162

TEST RESULTS - FUEL/AIR RATIO VS DISTANCE FROM TOP OF TANK

TESTNO	5	JMAX 9	ACAL	88	PCAL 14.70	PTEST 14.70				
TIME/DIST	1	4	7	10	13	16	19	22	25	28
0.00 PRESF	.996									
F/AIR	.1810									
.25 PRESF	.912	.943	.912							
F/AIR	.1648	.1708	.1648							
.50 PRESF	.755	.839	.860	.943						
F/AIR	.1348	.1507	.1547	.1708						
.75 PRESF	.629	.702	.734	.818	.839	.912				
F/AIR	.1113	.1250	.1309	.1467	.1507	.1648				
1.00 PRESF	.629	.650	.650	.650	.734	.786	.996			
F/AIR	.1113	.1152	.1152	.1152	.1309	.1407	.1810			
1.25 PRESF	.598	.598	.629	.655	.655	.681	.786	.839		
F/AIR	.1055	.1055	.1113	.1162	.1162	.1211	.1407	.1507		
1.50 PRESF	.598	.598	.598	.598	.598	.629	.681	.839	.912	1.017
F/AIR	.1055	.1055	.1055	.1055	.1055	.1113	.1211	.1507	.1648	.1851
1.75 PRESF	.524	.524	.545	.545	.608	.608	.629	.786	.943	.943
F/AIR	.0921	.0921	.0959	.0959	.1075	.1075	.1113	.1407	.1708	.1708

TEST RESULTS - FUEL/AIR RATIO VS DISTANCE FROM TOP OF TANK

TESTNO A JMAX R ACAL BB PCAL 14.70 PTEST 14.70

TIME/DIST		1	4	7	10	13	16	19	22	25	28
0.00	PRESF	2.359									
	F/AIR	.4760									
.25	PRESF	1.939	2.097	2.359							
	F/AIR	.3785	.4143	.4760							
.50	PRESF	1.572	1.572	2.254	2.306						
	F/AIR	.2983	.2983	.4510	.4635						
.75	PRESF	1.415	1.415	2.097	2.254	2.464					
	F/AIR	.2653	.2653	.4143	.4510	.5014					
1.00	PRESF	1.572	1.415	1.939	2.359	2.359	2.359	2.359			
	F/AIR	.2983	.2653	.3785	.4760	.4760	.4760	.4760			
1.25	PRESF	1.153	1.310	1.625	1.835	1.939	2.097	2.097	2.097		
	F/AIR	.2120	.2438	.3095	.3552	.3785	.4143	.4143	.4143		
1.50	PRESF	1.153	1.153	1.677	1.939	2.044	2.097	2.097	2.097	2.097	2.097
	F/AIR	.2120	.2120	.3208	.3785	.4023	.4143	.4143	.4143	.4143	.4143

TEST RESULTS - FUEL/AIR RATIO VS DISTANCE FROM TOP OF TANK

TESTNO 7 JMAX 8 ACAL 88 PCAL 14.70 PTEST 7.31

TIME/DIST		1	3	7	10	13	16	19	22	25
0 00	PRESF	.964								
	F/AIR	.3786								
.25	PRESF	.964	1.048	.964						
	F/AIR	.3786	.4170	.3786						
.50	PRESF	1.048	1.027	1.048	1.038					
	F/AIR	.4170	.4073	.4170	.4121					
.75	PRESF	1.048	.996	1.027	1.048					
	F/AIR	.4170	.3928	.4073	.4170					
1.00	PRESF	1.447	1.415	1.363	1.363	1.279	1.279	1.279		
	F/AIR	.6145	.5986	.5708	.5708	.5282	.5282	.5282		
1.25	PRESF	1.258	1.258	1.258	1.164	1.143	1.048	1.101	1.048	
	F/AIR	.5177	.5177	.5177	.4715	.4615	.4170	.4415	.4170	
1.50	PRESF	.996	1.258	1.258	1.258	1.153	1.122	1.153	1.153	
	F/AIR	.3928	.5177	.5177	.5177	.4665	.4515	.4665	.4665	

TEST RESULTS - FUEL/AIR RATIO VS DISTANCE FROM TOP OF TANK

TESTNO	R JMAX	R ACAL	RR PCAL	14.70 PTEST	12.74					
TIME/DIST	1	3	7	10	13	16	19	22	25	28
0.00 PRESF	.964									
F/AIR	.2040									
.25 PRESF	.964	1.101	1.101	1.101						
F/AIR	.2040	.2355	.2355	.2355						
.50 PRESF	.860	.860	.860	.860	.891					
F/AIR	.1802	.1802	.1802	.1802	.1873					
.75 PRESF	.954	.860	.860	.912	1.027	1.027				
F/AIR	.2016	.1802	.1802	.1921	.2185	.2185				
1.00 PRESF	.860	.860	.860	.860	.891	.891	.912	.964		
F/AIR	.1802	.1802	.1802	.1802	.1873	.1873	.1921	.2040		
1.25 PRESF	.839	.839	.839	.839	.839	.839	.860	.943	.943	.943
F/AIR	.1755	.1755	.1755	.1755	.1755	.1755	.1802	.1992	.1992	.1992
1.50 PRESF	.514	.514	.514	.524	.629	.734	.734	.786	.786	.839
F/AIR	.1046	.1046	.1046	.1069	.1294	.1522	.1522	.1638	.1638	.1755

TEST RESULTS - FUEL/AIR RATIO VS DISTANCE FROM TOP OF TANK

TESTNO	9	JMAX	8	ACAL	88	PCAL	14.70	PTEST	14.70			
TIME/DIST	1	3	7	10	13	16	19	22	25	28		
0.00 PRESF	.839											
F/AIR	.1507											
.25 PRESF	.755	.755	.839	.839								
F/AIR	.1348	.1348	.1507	.1507								
.50 PRESF	.629	.734	.807	.807	.807							
F/AIR	.1113	.1309	.1447	.1447	.1447							
.75 PRESF	.650	.702	.755	.755	.755	.755						
F/AIR	.1152	.1250	.1348	.1348	.1348	.1348						
1.00 PRESF	.629	.681	.755	.786	.786	.786						
F/AIR	.1113	.1211	.1348	.1407	.1407	.1407						
1.25 PRESF	.608	.608	.671	.734	.786	.786	.786	.786				
F/AIR	.1075	.1075	.1191	.1309	.1407	.1407	.1407	.1407				
1.50 PRESF	.713	.419	.440	.524	.577	.598	.681	.734	.765	.818		
F/AIR	.1269	.0731	.0769	.0921	.1017	.1055	.1211	.1309	.1368	.1467		

TEST RESULTS - FUEL/AIR RATIO VS DISTANCE FROM TOP OF TANK

TESTNO	10 JMAX	5 ACAL	88 PCAL	14.70 PTEST	12.70				
TIME/DIST	1	4	7	10	13	16	19	22	25	28
0.00 PRESF	.734									
F/AIR	.1527									
.25 PRESF	.545	.545	.619	.629	.629	.629				
F/AIR	.1117	.1117	.1275	.1298	.1298	.1298				
.50 PRESF	.577	.577	.608	.608	.608	.608	.608	.608		
F/AIR	.1185	.1185	.1252	.1252	.1252	.1252	.1252	.1252		
.75 PRESF	.577	.598	.629	.629	.598	.629	.629	.629		
F/AIR	.1185	.1230	.1298	.1298	.1230	.1298	.1298	.1298		

TEST RESULTS - FUEL/AIR RATIO VS DISTANCE FROM TOP OF TANK

TESTNO 11 JMAX 9 ACAL 88 PCAL 14.70 PTEST 14.70

TIME/DIST		1	4	7	10	13	16	19	22	25	28
0.00	PRESS	1.048									
	F/AIR	.1913									
.25	PRESS	.912	1.027	1.069							
	F/AIR	.1668	.1871	.1954							
.50	PRESS	.839	.943	1.122	1.153						
	F/AIR	.1507	.1708	.2058	.2120						
.75	PRESS	.755	.858	.943	1.174	1.258					
	F/AIR	.1348	.1467	.1708	.2162	.2331					
1.00	PRESS	.598	.629	.912	.943	1.153	1.174				
	F/AIR	.1055	.1113	.1648	.1708	.2120	.2162				
1.25	PRESS	.598	.650	.713	.943	.996	1.185	1.206			
	F/AIR	.1055	.1152	.1269	.1708	.1810	.2183	.2225			
1.50	PRESS	.577	.629	.713	.839	.891	1.048	1.153	1.310		
	F/AIR	.1017	.1113	.1269	.1507	.1607	.1913	.2120	.2438		
1.75	PRESS	.472	.534	.681	.713	.765	.985	1.048	1.153	1.248	
	F/AIR	.0826	.0921	.1211	.1269	.1368	.1790	.1913	.2120	.2310	

TEST RESULTS - FUEL/AIR RATIO VS DISTANCE FROM TOP OF TANK

TESTNO	12	JMAX	7	ACAL	88	PCAL	14.70	PTEST	14.70				
TIME/DIST	1		3	7	10	13	16	19	22	25	28		
0.00 PRESF	.943												
F/AIR	.1708												
.25 PRESF	.440	.650	.681	.839	.891								
F/AIR	.0769	.1152	.1211	.1507	.1607								
.50 PRESF	.314	.440	.524	.629	.839	.902							
F/AIR	.0545	.0769	.0921	.1113	.1507	.1627							
.75 PRESF	.314	.367	.498	.598	.681	.702	.870						
F/AIR	.0545	.0638	.0873	.1055	.1211	.1250	.1567						
1.00 PRESF	.283	.325	.482	.524	.629	.702	.912	.943					
F/AIR	.0489	.0563	.0845	.0921	.1113	.1250	.1648	.1708					
1.25 PRESF	.262	.367	.419	.440	.545	.545	.776	.839	1.017	1.048			
F/AIR	.0452	.0638	.0731	.0769	.0959	.0959	.1388	.1507	.1851	.1913			

TEST RESULTS - FUEL/AIR RATIO VS DISTANCE FROM TOP OF TANK

TESTNO 13 JMAX 8 ACAL BB PCAL 14.70 PTEST 14.70

TIME/DIST		1	3	7	10	13	16	19	22	25	28
0.00	PRESF	1.048									
	F/AIR	.1913									
.25	PRESF	.629	.788	1.048							
	F/AIR	.1113	.1467	.1913							
.50	PRESF	.577	.577	.755	.807	1.048					
	F/AIR	.1017	.1017	.1348	.1447	.1913					
.75	PRESF	.461	.524	.681	.912	.964	1.143				
	F/AIR	.0807	.0931	.1211	.1648	.1749	.2099				
1.00	PRESF	.388	.419	.629	.734	.912	1.048	1.122			
	F/AIR	.0675	.0731	.1113	.1309	.1648	.1913	.2058			
1.25	PRESF	.388	.419	.440	.608	.818	.891	.943	1.048		
	F/AIR	.0675	.0731	.0769	.1075	.1467	.1607	.1708	.1913		
1.50	PRESF	.294	.388	.440	.503	.639	.818	.891	1.027	1.048	
	F/AIR	.0507	.0694	.0769	.0883	.1133	.1467	.1607	.1871	.1913	

TEST RESULTS - FUEL/AIR RATIO VS DISTANCE FROM TOP OF TANK

TESTNO 14 JMAX 8 ACAL 88 PCAL 14.70 PTEST 14.70

TIME/DIST		1	3	7	10	13	16	19	22	25	28
0.00	PRESF	1.887									
	F/AIR	.3668									
.25	PRESF	1.835	1.835	1.887	1.887						
	F/AIR	.3552	.3552	.3668	.3668						
.50	PRESF	1.835	1.835	1.704	1.835	1.887	1.887				
	F/AIR	.3552	.3552	.3265	.3552	.3668	.3668				
.75	PRESF	1.835	1.835	1.782	1.835	1.835	1.835	1.966			
	F/AIR	.3552	.3552	.3436	.3552	.3552	.3552	.3844			
1.00	PRESF	1.835	1.704	1.704	1.704	1.835	1.835	1.835	1.835		
	F/AIR	.3552	.3265	.3265	.3265	.3552	.3552	.3552	.3552		
1.25	PRESF	1.704	1.835	1.704	1.704	1.704	1.704	1.704	1.835	1.704	
	F/AIR	.3265	.3552	.3265	.3265	.3265	.3265	.3265	.3552	.3265	
1.50	PRESF	1.704	1.835	1.572	1.704	1.704	1.704	1.704	1.704	1.704	1.704
	F/AIR	.3265	.3552	.2983	.3265	.3265	.3265	.3265	.3265	.3265	.3265

TEST RESULTS - FUEL/AIR RATIO VS DISTANCE FROM TOP OF TANK

TESTNO 16 JMAX 8 ACAL 88 PCAL 14.70 PTEST 14.70

TIME/DIST		1	3	7	10	13	16	19	22	25	28
0.00	PRESF	1.704	1.966								
	F/AIR	.3265	.3844								
.25	PRESF	1.572	1.625	1.572	1.494						
	F/AIR	.2983	.3095	.2983	.2817						
.50	PRESF	1.572	1.572	1.415	1.468	1.572					
	F/AIR	.2983	.2983	.2653	.2763	.2983					
.75	PRESF	1.572	1.572	1.441	1.441	1.468	1.468	1.572			
	F/AIR	.2983	.2983	.2708	.2708	.2763	.2763	.2983			
1.00	PRESF	1.415	1.415	1.468	1.468	1.494	1.441	1.389	1.572	1.572	
	F/AIR	.2653	.2653	.2763	.2763	.2817	.2708	.2599	.2983	.2983	
1.25	PRESF	1.310	1.494	1.494	1.310	1.363	1.494	1.572	1.310	1.441	
	F/AIR	.2438	.2817	.2817	.2438	.2545	.2817	.2983	.2438	.2708	
1.50	PRESF	1.494	1.363	1.363	1.363	1.441	1.441	1.441	1.441	1.494	
	F/AIR	.2817	.2545	.2545	.2545	.2708	.2708	.2708	.2708	.2817	

TEST RESULTS - FUEL/AIR RATIO VS DISTANCE FROM TOP OF TANK

TESTNO 17 JMAX 5 ACAL 88 PCAL 14.70 PTEST 14.70

TIME/DIST		1	4	7	10	13	16	19	22	25	28
0.00	PRESF	1.048									
	F/AIR	.1913									
.25	PRESF	.734	.839	.943	.943						
	F/AIR	.1309	.1507	.1708	.1708						
.50	PRESF	.755	.891	.891	.891						
	F/AIR	.1348	.1607	.1607	.1607						
.75	PRESF	.786	.912	.891	.902	.902	1.017				
	F/AIR	.1407	.1648	.1607	.1627	.1627	.1851				

TEST RESULTS - FUEL/AIR RATIO VS DISTANCE FROM TOP OF TANK

TESTNO	18	JMAX	8	ACAL	88	PCAL	14.70	PTEST	14.70				
TIME/DIST	1		4		7	10	13	16	19	22	25	28	
0.00 PRESF	.776												
F/AIR	.1388												
.25 PRESF	.514		.671		.755	.881							
F/AIR	.0902		.1191		.1348	.1587							
.50 PRESF	.419		.503		.650	.891	.912						
F/AIR	.0731		.0883		.1152	.1607	.1648						
.75 PRESF	.231		.356		.482	.629	.797	.912					
F/AIR	.0397		.0619		.0845	.1113	.1427	.1648					
1.00 PRESF	.262		.283		.388	.472	.598	.765	.839	.954			
F/AIR	.0452		.0489		.0675	.0826	.1055	.1368	.1507	.1729			
1.25 PRESF	.199		.210		.262	.388	.461	.608	.692	.776	.912	.923	
F/AIR	.0342		.0360		.0452	.0675	.0807	.1075	.1230	.1388	.1648	.1668	
1.50 PRESF	.126		.178		.262	.283	.377	.430	.556	.734	.786	.870	
F/AIR	.0213		.0306		.0452	.0489	.0656	.0750	.0978	.1309	.1407	.1567	

TEST RESULTS - FUEL/AIR RATIO VS DISTANCE FROM TOP OF TANK

TESTNO 19	JMAX	R	ACAL	88	PCAL	14.70	PTEST	14.70			
TIME/DIST	1	4	7	10	13	16	19	22	25	28	
0.00 PRESF	.839										
F/AIR	.1507										
.25 PRESF	.839	.891	.943	.996							
F/AIR	.1507	.1607	.1708	.1810							
.50 PRESF	.419	.482	.734	.797	.943	1.006					
F/AIR	.0731	.0845	.1309	.1427	.1708	.1830					
.75 PRESF	.283	.419	.508	.650	.755	.943	1.017	1.122			
F/AIR	.0489	.0731	.0892	.1152	.1348	.1708	.1851	.2058			
1.00 PRESF	.262	.293	.388	.493	.692	.734	.839	.912	1.017		
F/AIR	.0452	.0489	.0675	.0864	.1230	.1309	.1507	.1648	.1851		
1.25 PRESF	.252	.273	.335	.419	.524	.629	.650	.765	.839	.943	
F/AIR	.0434	.0471	.0582	.0731	.0921	.1113	.1152	.1368	.1507	.1708	
1.50 PRESF	.262	.283	.314	.419	.419	.503	.566	.723	.734	.891	
F/AIR	.0452	.0489	.0545	.0731	.0731	.0883	.0998	.1289	.1309	.1607	

TEST RESULTS - FUEL/AIR RATIO VS DISTANCE FROM TOP OF TANK

TESTNO 20 JMAX 6 ACAL 88 PCAL 14.70 PTEST 14.70

TIME/DIST		1	3	7	10	13	16	19	22	25	28
0 00	PRESF	.786									
	F/AIR	.1407									
.25	PRESF	.577	.755	.860	.985						
	F/AIR	.1017	.1348	.1547	.1790						
.50	PRESF	.388	.419	.577	.807	.943	1.017				
	F/AIR	.0675	.0731	.1017	.1447	.1708	.1851				
.75	PRESF	.294	.335	.430	.629	.713	.839	.964	1.017		
	F/AIR	.0507	.0582	.0750	.1113	.1269	.1507	.1749	.1851		
1.00	PRESF	.231	.293	.377	.493	.577	.681	.776	.881	.996	
	F/AIR	.0397	.0489	.0656	.0864	.1017	.1211	.1388	.1587	.1810	

TEST RESULTS - FUEL/AIR RATIO VS DISTANCE FROM TOP OF TANK

TESTNO 21A JMAX 4 ACAL 88 PCAL 14.70 PTEST 14.70

TIME/DIST		1	3	7	10	13	16	19	22	25	28
0 00	PRESF	1.101									
	F/AIR	.2016									
.25	PRESF	1.127	1.127	.655	1.048						
	F/AIR	.2068	.2068	.1162	.1913						
.50	PRESF	1.572	1.572	.655	.655	.734	1.048				
	F/AIR	.2983	.2983	.1162	.1162	.1309	.1913				

TEST RESULTS - FUEL/AIR RATIO VS DISTANCE FROM TOP OF TANK

TESTNO 22A JMAX 6 ACAL 88 PCAL 14.70 PTEST 14.70

TIME/DIST		1	3	7	10	13	16	19	22	25	28
0 00	PRESF	1.625									
	F/AIR	.3095									
.25	PRESF	1.704	1.704	1.232	1.310						
	F/AIR	.3265	.3265	.2278	.2438						
.50	PRESF	1.572	.917	.786	.917	1.101	1.310				
	F/AIR	.2983	.1658	.1407	.1658	.2016	.2438				
.75	PRESF	.577	.472	.472	.577	.786	.970	1.206	1.546		
	F/AIR	.1017	.0826	.0826	.1017	.1407	.1759	.2225	.2928		
1.00	PRESF	1.494	1.572	1.572	.786	.629	.708	1.048	1.179	1.389	
	F/AIR	.2817	.2983	.2983	.1407	.1113	.1260	.1913	.2173	.2599	

TEST RESULTS - FUEL/AIR RATIO VS DISTANCE FROM TOP OF TANK

TESTNO 23 JMAX 5 ACAL 88 PCAL 14.70 PTEST 14.70

TIME/DIST		1	3	7	10	13	16	19	22	25	28
0 00	PRESF	1.441									
	F/AIR	.2708									
.25	PRESF	1.572	1.572	1.572	1.179	1.310					
	F/AIR	.2983	.2983	.2983	.2173	.2438					
.50	PRESF	1.520	.655	.629	.681	.839	1.179	1.441			
	F/AIR	.2873	.1162	.1113	.1211	.1507	.2173	.2708			
.75	PRESF	1.441	.786	.577	.524	.734	.839	1.179	1.310		
	F/AIR	.2708	.1467	.1017	.0921	.1309	.1507	.2173	.2438		

APPENDIX II

EFFECT OF JET FUELS (JP-4) AND EMULSION ON FUEL TANK LINER MATERIAL

Some test runs made after the installation of the tank liner showed little or no fuel/air ratio change throughout the entire test (see tests 14 and 16). Equipment failure was first suspected, and the sampling lines and the chromatograph were checked for leaks or malfunction. The test equipment was found to be in order. Since it is quite common for the plasticising components in synthetic rubbers to migrate, it was thought that perhaps such a phenomenon was occurring and that this could be having some effect on the measured composition profiles. The manufacturer of the lining material was contacted, and saturation data for their PF-10056 synthetic rubber/nylon liner material were obtained. It indicated that the weight losses after soaking the material 7 days in JP-4 varied from 2.0% to 7.0%.

The loss in weight is due to the fact that the aromatic plasticer in the rubber liner diffuses and changes place with the aromatic fractions (up to 25%) within the JP-4. The aromatics in the fuel are lighter than those in the PF-10056; thus the loss in weight. This phenomenon also accounts for the saturation of the PF-10056 with some components of JP-4 fuel.

Laboratory tests were run at Dynamic Science to verify the information received from the manufacturer. These tests are described in the following paragraphs.

TEST PROCEDURE

Two-inch squares of PF-10056 were weighed and placed in JP-4 and emulsified fuel at ambient temperature and in JP-4 at 90° F. Samples were removed from the ambient temperature media at 24-hour intervals over a 72-hour period and were reweighed. Samples in the 90° F test media were reweighed at 24-, 48-, and 72-hour and 1-week intervals. All samples showed a significant weight loss, as shown in the following tables:

TABLE II. JP-4 FUEL AT AMBIENT TEMPERATURE				
Date	Time (hours)	Sample Weight(grams)		
		Sample 1	Sample 2	Sample 3
1-6-70	0	2.6588	2.6050	2.6089
1-7-70	24	2.6466	-	-
1-8-70	48	-	2.5825	-
1-9-70	72	-	-	2.5824
Weight Change (gms)		0.0122	0.0225	0.0265
Weight Change (%)		0.458%	0.864%	1.015%

TABLE III. EMULSIFIED FUEL AT AMBIENT TEMPERATURE				
Date	Time (hours)	Sample Weight (grams)		
		Sample 1	Sample 2	Sample 3
1-6-70	0	2.7070	2.7041	2.6478
1-7-70	24	2.6611	-	-
1-8-70	48	-	2.6559	-
1-9-70	72	-	-	2.5948
Weight Change (gms)		0.0459	0.0482	0.0530
Weight Change (%)		1.695%	1.782%	2.00%

TABLE IV. JP-4 FUEL AT 90°F

Date	Time (hours)	Sample Weight (grams)			
		Sample 1	Sample 2	Sample 3	Sample 4
1-12-70	0	2.6350	2.6638	2.7221	2.7732
1-13-70	24	2.5600	-	-	-
1-14-70	48	-	2.5668	-	-
1-15-70	72	-	-	2.6216	-
1-19-70	1 Week	-	-	-	2.6657
Weight Change (gms)		0.0750	0.0970	0.1005	0.1075
Weight Change (%)		2.84	3.64	3.69	3.87

APPENDIX III

DEAERATION OF JP-4 FUEL

Deaeration of JP-4 fuel was observed in the form of gas bubbles during setting of tank pressure during the testing. This flow of gas bubbles saturated with fuel vapors can lead to a bulk convection into the ullage space and a lessening of degree of mixture of fuel/air gradients within the ullage. To define the extent of air dissolution, a small chemical analysis program was initiated. Samples of the Standard JP-4 fuel, MIL-T-5624G, shipped in 50-gallon batches (55-gallon drums), were taken from an unused drum of fuel. Mass spectrometer analysis was taken to analyze the composition of dissolved gases in the fuel as received and after holding at 1/2 atmosphere for 2 hours (mixture was at equilibrium with the 1/2 atmosphere after this period).

TEST PROCEDURES

The solubilities of dissolved gas were experimentally determined by desorbing and measuring the gas dissolved in a known volume of fuel (apparatus shown in Figure 25). For the samples saturated under a pressure of 1 atmosphere of air, the fuel was introduced through nylon tubing into a 92.95-ml ampoule, which was filled completely and closed off by a stopcock. This ampoule was connected to a high-vacuum system, and the connecting lines above the stopcock were evacuated to $<10^{-4}$ mm Hg. Then the stopcock was opened and the gases and fuel vapors were allowed to expand into a 2-l trap cooled to $\approx -60°C$ to condense the majority of the fuel. The noncondensible gases were passed through three liquid-nitrogen-cooled traps to remove traces of volatile fuel components and were then collected in a Sprengel pump (Reference 5). During collection of the gases, the ampoule containing the fuel was heated to $\approx 70°C$ to facilitate distillation. After the volume of the noncondensibles was measured, the gases were transferred into another ampoule and analyzed by mass spectroscopy. The mass spectrometer was calibrated for N_2, O_2, and Ar before analysis.

To obtain a fuel sample saturated with air at ≈ 0.5 atm, ≈ 200 ml of fuel (saturated with air at atmospheric pressure) was placed in a 250-ml round-bottom flask attached to a glass-T equipped with a stopcock for evacuation. The 92.95-ml ampoule was attached to the second arm of the glass-T, and the whole system was connected to a vacuum line. The total pressure in the system was then reduced to ≈ 0.5 atm and kept under this condition for 105 min while the fuel was stirred. During the last 20 min of this period, the pressure above the fuel remained constant at 385.7 mm Hg. The fuel to be analyzed was then transferred into the measured volume by tipping the whole system. The measurement of the dissolved gases was subsequently carried out as described in the preceding paragraph.

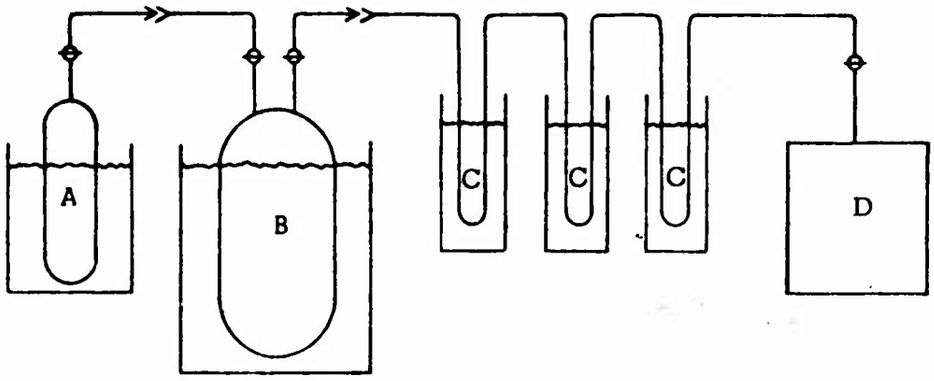

A = 92.95-ml ampoule heated during distillation to ≈ 70°C
B = 2-l trap cooled to ≈ - 60°C
C = liquid-nitrogen-cooled u-traps
D = Sprengel pump
⊖ = glass stopcocks
>> = pairs of ground glass joints

Figure 25. Experimental Arrangement for Measuring Gases Dissolved in JP-4 Fuel.

To check the effect of temperature on the solubility of "air" in JP-4 fuel, the amounts of gases dissolved under an air pressure of 1 atmosphere were measured at two different temperatures (19.7°C and 23.2°C). The results differed by not more than ± 1.14% of the amounts dissolved, which shows that the temperature coefficient of the solubility of oxygen and nitrogen in JP-4 fuel is negligibly small within the above temperature range. Temperature has an equally small effect upon density within the range of from 19.7°C to 24.1°C. Four measurements showed the density of the JP-4 fuel sample to vary within the limits 0.754 ± 0.004 g/ml.

The results of the determination of N_2, O_2, and Ar dissolved in JP-4 fuel under specified conditions of temperature and air pressure are compiled in Table V. Also included in Table V are the sums of dissolved nitrogen and oxygen to make comparison with available data on dissolved "air" possible. In addition, the ratio of dissolved nitrogen to oxygen is listed and compared with the same ratio in air.

From Table V it can also be seen that the ratio of nitrogen to oxygen in the solution is lower than the ratio of the two gases in air. This indicates that oxygen is more soluble in JP-4 than nitrogen, in agreement with the observations of Polishuk, et al (Reference 6). Naturally, the nitrogen to oxygen ratio in the gas coming out of the solution must be the same as that in the original solution since, during decrease of pressure over the solution, the ratio of the partial pressures has not been changed. Calculating the N_2/O_2 ratio of the liberated gases from Table VI gives 2.194, in agreement with the N_2/O_2 ratios listed in Table VI for the gas remaining in solution.

The data of Table V are insufficient to evaluate the applicability of Henry's law to the system JP-4 fuel/air. However, the values obtained for the solubility at ≈0.5 atm and the average of the values measured at 1.0 atm would make it appear that Henry's law is not too closely followed. From Table V it can be calculated that upon decrease of pressure to 50.75% of 1 atm (385.7 mm Hg), the amount of oxygen remaining in solution was only 48.60% of the amount dissolved at 1 atm. When scaled to a 100-gal tank, this represents a significant oxygen addition to the vapor phase. The corresponding amount for nitrogen is 48.63%. It is believed that these differences (50.75% versus 48.6%) are an indication that Henry's law is not strictly followed, but that solubility (within the temperature range investigated) increases more with increasing pressure than would be predicted.

TABLE V. GASES DISSOLVED IN JP-4 FUEL
(At 1 Atmosphere and 1/2 Atmosphere)

p [mm Hg]	t (°C)	$[ml_{STP}/ml_{fuel}]$ N_2	O_2	Ar	N_2+O_2	Ratio N_2/O_2
≈760	19.7	0.10427	0.04810	0.00265	0.15237	2.168
≈760	23.2	0.10455	0.04703	0.00244	0.15158	2.223
Average	≈1 atm	0.10442	0.04757	0.00255	0.15198	2.195
385.7	24.1	0.05078	0.02312	0.00131	0.07390	2.196
Air	-	-	-	-	-	3.727

As calculated from Table V, the amounts of gases liberated from the JP-4 solution during reduction of the air pressure above the solution from 1 atmosphere to 0.5075 atmosphere are as listed in Table VI.

TABLE VI. AMOUNT OF GASES COMING OUT OF JP-4 SOLUTION DURING AIR PRESSURE DECREASE FROM 1 atm to 0.5075 atm

Gas	ml_{STP} set free per ml of fuel
N_2	0.05364
O_2	0.02445
Ar	0.00124
N_2+O_2	0.07808

Note: Task #1 Nominal - 100 gal=79×10^8ml

APPENDIX IV

DIFFUSION INDUCED CONVECTION OF HIGH VOLATILITY FUELS

(EXCERPT FROM KRIETH, "PRINCIPLES OF HEAT TRANSFER")

Mass transfer by molecular diffusion can be examined in an analogy-to-conduction-to-heat transfer. Mass transfer by molecular diffusion may occur in a stagnant fluid or in a fluid in laminar flow. The transient one-dimensional mass-transfer equation can be written in a form identical to the Fourier heat-transfer equation,

$$\frac{\partial c_a}{\partial \theta} = D_v \frac{\partial^2 c_a}{\partial y^2}$$

where c_a =concentration of component A in a mixture of A and B, lb-moles/cu ft

θ =time, hr

D_v =mass diffusivity, sq ft/hr

y =distance in the direction of diffusion, ft

In the steady state, the concentration at any point does not vary with time, and

$$\frac{N_a}{A} = - D_v \frac{dc_A}{dy}$$

where N_a/A is the mass flux in lb-moles/hr sq ft. The negative sign appears because the concentration gradient is negative in the direction of mass transfer.

The above equation states that mass will be transferred between two points in a fluid if a difference in concentration exists between the points. Mass transfer occurs at an appreciable rate only in gases and liquids. In solids, mass transfer is suppressed by the relative immobility of the molecules.

In the gas phase, concentrations are usually expressed as partial pressures. If the perfect gas law,

$$p_a = \frac{n_a \mathcal{R} T}{V} = c_a \mathcal{R} T$$

where p_a = partial pressure of gas A in a mixture, atm

n_a = number of moles of gas, lb-moles

$\mathcal{R}$ = gas constant, cu ft atm/lb-mole F

V = gas volume, cu ft

is assumed to hold, the above equation becomes

$$\frac{N_a}{V} = \frac{-D_v}{\mathcal{R}T} \frac{dp_a}{dy}$$

Integration between any two planes in the fluid gives

$$\frac{N_a}{V} = \frac{-D_v(p_{a_2} - p_{a_1})}{\mathcal{R}T(y_2 - y_1)}$$

where p_{a_1} is the partial pressure at y_1 and p_{a_2} is the partial pressure at y_2. The above equation is rigorously correct only for equimolar counter diffusion. In equimolar counter diffusion, gases A and B diffuse simultaneously in opposite directions through each other. The rates of diffusion are equal but in opposite directions, i.e., $N_a = -N_b$.

Diffusion of a gas through a second stationary gas often occurs in practical equipment. For example, in the humidification of air, water vapor must diffuse from the air-water interface through an air layer which is essentially stationary (as is the case in fuel tank diffusion). Conversely, in the dehumidification of air, water vapor must diffuse from the bulk of the gas phase through stationary air to reach the surface at which it condenses.

Consider the case of gas A diffusing through a stationary gas B from a gas-liquid interface where gas A leaves the volume. Gas B diffuses toward the interface but is essentially insoluble. Since A diffuses away from the interface, there must be a partial pressure gradient for A in the direction of diffusion. The rate of transfer of A is given by

$$\frac{N_a}{A} = \frac{-D_v}{\mathcal{R}T} \frac{dp_a}{dy}$$

Since there is a continuous gas phase, the total pressure P must be constant throughout the gas. Since $p_a + p_b = P$, a gradient in p_a will cause a gradient of p_b in the opposite direction. This gradient will force diffusion of gas B toward the interface, at the rate

$$\frac{N_b}{A} = \frac{-D_v}{\mathcal{R}T} \frac{dp_b}{dy} = \frac{D_v}{\mathcal{R}T} \frac{dp_a}{dy}$$

since $dp_b/dy = -dp_a/dy$. Since gas B is not being absorbed at a high rate at the interface, even though it is diffusing toward the interface, some other mechanism must transport gas B to maintain a constant concentration of gas B at the interface. A bulk flow of gas away from the interface sweeps the gas B which is diffusing toward it. The bulk flow will consist of a mixture of A and B.

This diffusion-induced convection occurs at higher liquid temperatures and lower pressure, and was supported by the experimental data in that composition profiles were flatter for these conditions.

Unclassified

Security Classification

DOCUMENT CONTROL DATA - R & D

(Security classification of title, body of abstract and indexing annotation must be entered when the overall report is classified)

1. ORIGINATING ACTIVITY (Corporate author) Dynamic Science, a Division of Marshall Industries 2400 Michelson Drive, Irvine, California 92664	2a. REPORT SECURITY CLASSIFICATION Unclassified 2b. GROUP

3. REPORT TITLE

FLIGHT VIBRATION AND ENVIRONMENTAL EFFECTS ON FORMATION OF COMBUSTIBLE MIXTURES WITHIN AIRCRAFT FUEL TANKS

4. DESCRIPTIVE NOTES (Type of report and inclusive dates)

Final Report (23 June 1969 through March 31, 1970)

5. AUTHOR(S) (First name, middle initial, last name)

Kosvic, T. C., Helgeson, N. L., and Breen, B. P.

6. REPORT DATE	7a. TOTAL NO. OF PAGES	7b. NO. OF REFS
September 1970	86	6

8a. CONTRACT OR GRANT NO.	9a. ORIGINATOR'S REPORT NUMBER(S)
DAAJ02-69-C-0063 b. PROJECT NO. Task 1F162203A15003 c. d.	USAAVLABS Technical Report 70-43 9b. OTHER REPORT NO(S) (Any other numbers that may be assigned this report) SN-162-F ✓

10. DISTRIBUTION STATEMENT

This document is subject to special export controls, and each transmittal to foreign governments or foreign nationals may be made only with prior approval of U. S. Army Aviation Materiel Laboratories, Fort Eustis, Virginia 23604.

11. SUPPLEMENTARY NOTES	12. SPONSORING MILITARY ACTIVITY
	U.S.Army Aviation Materiel Laboratories Fort Eustis, Virginia

13. ABSTRACT

The objective of this study was to determine fuel tank vapor space characteristics for a simulated helicopter fuel tank and to evaluate the potential hazard which exists. Fuel/air ratios were measured as a function of time and position within the ullage of the fuel tank for specified flight profiles. These results were compared to published flammability limits as a basis for assessing flight hazard potential. The flight profiles were simulated by withdrawing fuel (at rated engine usage) from a vibrating tank held at constant pressure and temperature. Parametric variations were made in fuel temperature (40° to 100°F), flight altitude (0 to 15,000 feet), vibration environment, and fuel properties (liquid JP-4 versus JP-4 emulsion EF4-104H). Another important variable not considered initially but which was uncovered during the course of this investigation was the effect that the rubberized tank liner could have on the measured fuel/air ratios. The extent of this effect was found to be related to fuel temperature and exposure time of the liner to the fuel.

The experimental results showed those ranges of the test variables which had a significant effect on the measured fuel/air ratios. They also demonstrated that fuel/air mixture gradients do exist in fuel tanks under flight conditions. It was found that tanks which would be considered safe as determined by calculations for equilibrium conditions actually contain flammable regions, even for level flight. An analytical model for the ullage space was written which included transient fuel vapor diffusion and convection which was brought about by venting of the ullage. The sample cases gave results which showed reasonable agreement in both shape and magnitude with the measured composition profiles.

DD FORM 1 NOV 68 1473 REPLACES DD FORM 1473, 1 JAN 64, WHICH IS OBSOLETE FOR ARMY USE.

Unclassified

Security Classification

Unclassified

Security Classification

14 KEY WORDS	LINK A		LINK B		LINK C	
	ROLE	WT	ROLE	WT	ROLE	WT
Fuel Tanks						
Vulnerability						
JP-4 Fuel						
EF4-104H						
Emulsified Fuel						
Fuel Tank Flight Simulator						
Aircraft Vibration						
Fuel Tank Ullage Gradients						

Unclassified

Security Classification

7633-70